

## Synthetic Approach to Readily Accessible Benzofuran-Fused BODIPY as Red-Emitting Laser Dyes

José L. Belmonte-Vázquez, Edurne Avellanal-Zaballa, Ernesto Enríquez-Palacios, Luis Cerdán, Ixone Esnal, Jorge Bañuelos, Clarisa Villegas-Gómez, Iñigo Lopez Arbeloa, and Eduardo Peña-Cabrera

*J. Org. Chem.*, **Just Accepted Manuscript** • DOI: 10.1021/acs.joc.8b02933 • Publication Date (Web): 31 Jan 2019

Downloaded from <http://pubs.acs.org> on February 1, 2019

### Just Accepted

“Just Accepted” manuscripts have been peer-reviewed and accepted for publication. They are posted online prior to technical editing, formatting for publication and author proofing. The American Chemical Society provides “Just Accepted” as a service to the research community to expedite the dissemination of scientific material as soon as possible after acceptance. “Just Accepted” manuscripts appear in full in PDF format accompanied by an HTML abstract. “Just Accepted” manuscripts have been fully peer reviewed, but should not be considered the official version of record. They are citable by the Digital Object Identifier (DOI®). “Just Accepted” is an optional service offered to authors. Therefore, the “Just Accepted” Web site may not include all articles that will be published in the journal. After a manuscript is technically edited and formatted, it will be removed from the “Just Accepted” Web site and published as an ASAP article. Note that technical editing may introduce minor changes to the manuscript text and/or graphics which could affect content, and all legal disclaimers and ethical guidelines that apply to the journal pertain. ACS cannot be held responsible for errors or consequences arising from the use of information contained in these “Just Accepted” manuscripts.

# Synthetic Approach to Readily Accessible Benzofuran-Fused BODIPY as Red-Emitting Laser Dyes

José L. Belmonte-Vázquez,<sup>†</sup> Edurne Avellanal-Zaballa,<sup>‡</sup> Ernesto Enríquez-Palacios,<sup>†</sup> Luis Cerdán,<sup>¥</sup> Ixone Esnal,<sup>‡</sup> Jorge Bañuelos,<sup>‡,\*</sup> Clarisa Villegas-Gómez,<sup>†</sup> Iñigo López Arbeloa,<sup>‡</sup> Eduardo Peña-Cabrera<sup>†,\*</sup>

<sup>†</sup> Departamento de Química. Universidad de Guanajuato, Noria Alta S/N. Guanajuato, Gto. Mexico 36050

<sup>‡</sup> Departamento de Química Física. Universidad del País Vasco-EHU, Apartado 644, 48080, Bilbao, Spain.

<sup>¥</sup> Instituto de Química-Física "Rocasolano", CSIC. Serrano 119, 28006 Madrid, Spain

Email: jorge.banuelos@ehu.eus, eduardop@ugto.mx

## Abstract

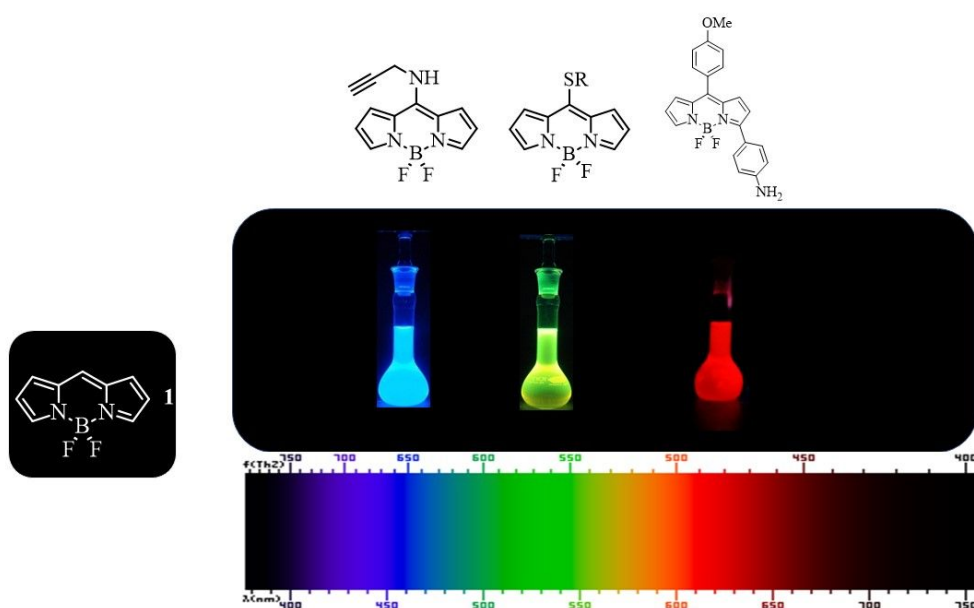
We took advantage of the chemoselective *meso*-functionalization 2,3,5,6-tetrabromo-8-methylthioBODIPY **6** to prepare a series of 2,3,5,6-tetrabromo-8-arylBODIPY derivatives suitable for  $S_NAr$  substitution reactions with phenols exclusively at the 3- and 5-positions. Pd(0)-catalyzed intramolecular arylation reaction ensued on the remaining brominated 2- and 6-positions to give a new family of benzofuran-fused BODIPY dyes. This method utilizes readily available starting materials and allows for the preparation of the title compounds with excellent functional group tolerance. Moreover, it was demonstrated that the methodology described herein is amenable for the incorporation of biomolecules. The photophysical and lasing properties of the benzofuran-fused BODIPY dyes were thoroughly analyzed with the aid of electrochemical measurements and quantum mechanical simulations. These dyes show

bright and intriguing emission (both fluorescence and laser) towards the red edge of the visible spectrum with remarkable tolerance under a strong and continuous irradiation.

## Introduction

Borondipyrromethenes (BODIPYs)<sup>1</sup> (Figure 1), are arguably some of the most versatile fluorophores there are.<sup>2</sup> Plenty has been written about their synthesis,<sup>3</sup> post-functionalization,<sup>4</sup> water solubility,<sup>5</sup> halogenated derivatives.<sup>6</sup> Similarly, there is vast information regarding their applications: in organic photovoltaic devices,<sup>7</sup> as components of novel light active materials,<sup>8</sup> as fluorescent tools,<sup>9</sup> as sensitizers for dye-sensitized solar cells,<sup>10</sup> as sensors for reactive oxygen species,<sup>11</sup> and in photodynamic therapy,<sup>12</sup> just to mention a few topics.

There are well-established fluorophores with a marked diversity of structures that emit at specific wavelengths.<sup>13</sup> However, the BODIPYs core structure is one of the few capable to fluoresce over the whole visible and near infrared (NIR) regions of the electromagnetic spectrum, if properly functionalized (Figure 1).<sup>2,14</sup>



1  
2  
3 **Figure 1.** Panchromatic properties of BODIPY dyes.

4 The possibility to induce a bathochromic shift on the optical properties of these dyes is highly  
5 desirable. Many imaginative attempts have been tested to design red-emitting BODIPYs.<sup>15</sup>  
6  
7 The reason of such search relies on the serious drawbacks of most of the available  
8 fluorophores in that spectral region for their optimal practical application.<sup>16</sup> As a matter of  
9 fact, cyanine dyes are able to provide spectral bands deep in the red edge, even reaching the  
10 NIR, but with low fluorescence efficiencies owing to their push-pull and conformationally  
11 flexible chromophores.<sup>17</sup> On the other hand, oxazine dyes render bright emission but are  
12 easily photobleached.<sup>18</sup> One way to circumvent such limitations is by shifting the spectral  
13 bands of BODIPYs, characterized by their excellent photophysics and robustness,<sup>2</sup> to the red  
14 edge thanks to the chemical versatility of its dipyrin core.<sup>4</sup> These red-emitting BODIPYs are  
15 used as building blocks to prepare polymers that can be used in photovoltaics, solar-cells,  
16 photodetectors, etc.<sup>19</sup> Such compounds find numerous applications in bio-medicine and  
17 related areas. Thus, NIR-emitting BODIPYs have been used as pH probes and in bio-  
18 imaging,<sup>20</sup> in photodynamic therapy,<sup>21</sup> and as molecular probes for reactive oxygen species  
19 (ROS).<sup>22</sup>

20  
21  
22  
23  
24  
25  
26  
27  
28  
29  
30  
31  
32  
33  
34  
35  
36  
37  
38  
39  
40  
41  
42  
43  
44  
45  
46  
47  
48  
49  
50  
51  
52  
53  
54  
55  
56  
57  
58  
59  
60  
A well-known approach to red-shift both absorption and emission of BODIPY dyes is to  
reduce their HOMO-LUMO gap by extending their conjugated system. Thus, the groups of  
Wu,<sup>23</sup> Rurack,<sup>24</sup> Jiao,<sup>25</sup> Okujima,<sup>26</sup> Ziessel,<sup>27</sup> Shinokubo,<sup>28</sup> Kubo,<sup>29</sup> among others, have  
reported a variety of different BODIPY structures featuring extended conjugated systems  
(Figure 2). Moreover, Wu and Ni have published a review with additional conjugated  
BODIPY structures.<sup>30</sup>

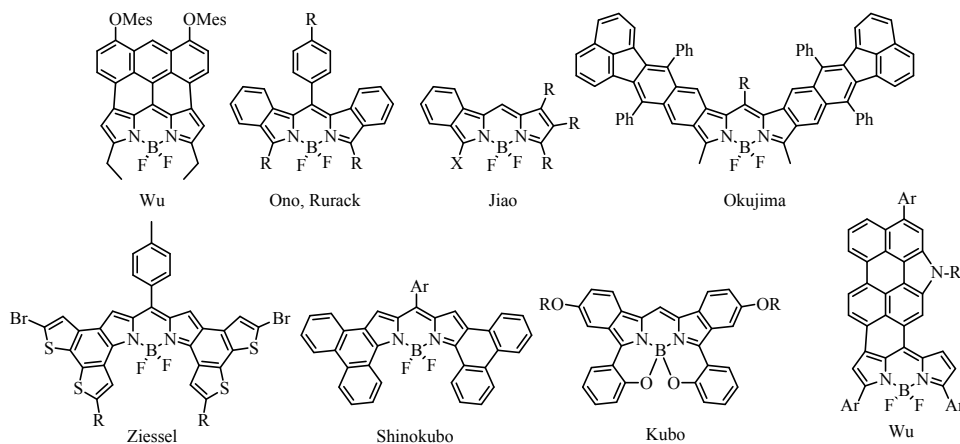
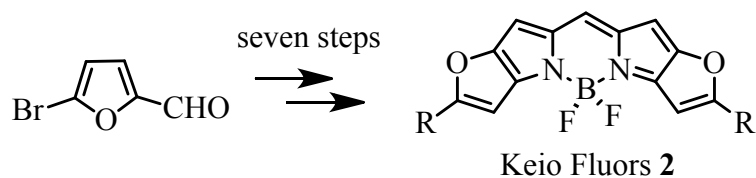


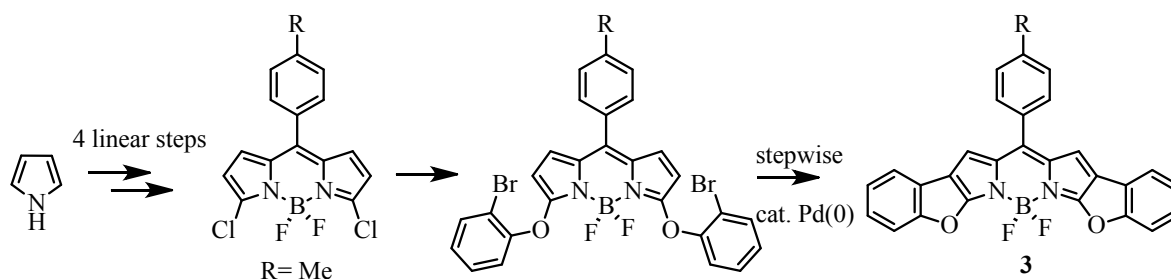
**Figure 2.** Representative examples of BODIPYs with extended conjugation.

The so-called Keio Fluors **2**, are BODIPY dyes with extension of the conjugation including heterocycles, specifically, furan. These feature results in dyes with improved properties, such as color tunability, sharp spectral bands, high extinction coefficients and fluorescence quantum yields. Additionally, they show little dependence of their brightness with solvent polarity. A significant disadvantage is that each derivative must be prepared by a linear synthesis comprising seven steps, leaving little or no room for further modifications of the final products (Scheme 1).<sup>31</sup>



**Scheme 1.** Linear synthesis of Keio Fluors

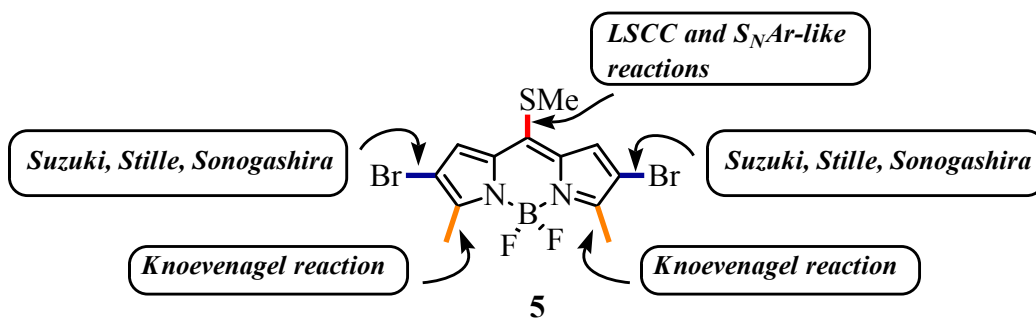
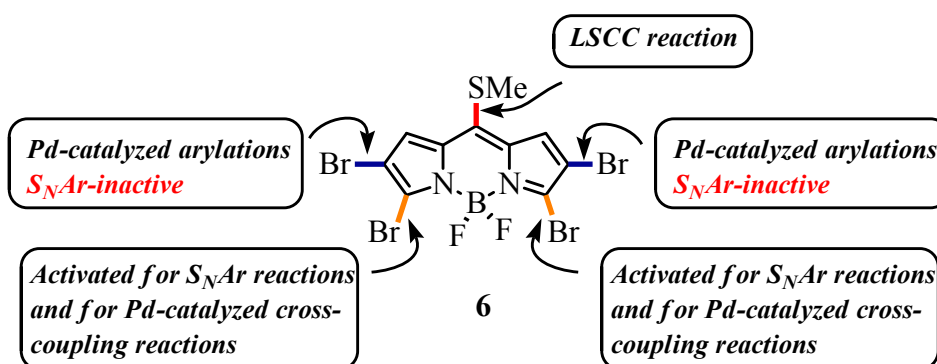
The synthesis of a single regioisomer **3** was described in 2010, using an alternative methodology (Scheme 2).<sup>32</sup>



### Scheme 2. Synthesis of BODIPY 3

After analyzing the synthetic sequence, one realizes that it becomes quite an undertaking to prepare different analogues for each of them would require repeating the whole process to vary the *meso*-substituent. Moreover, the introduction of additional functional groups on the benzofuran system would need a substituted *o*-bromophenol.

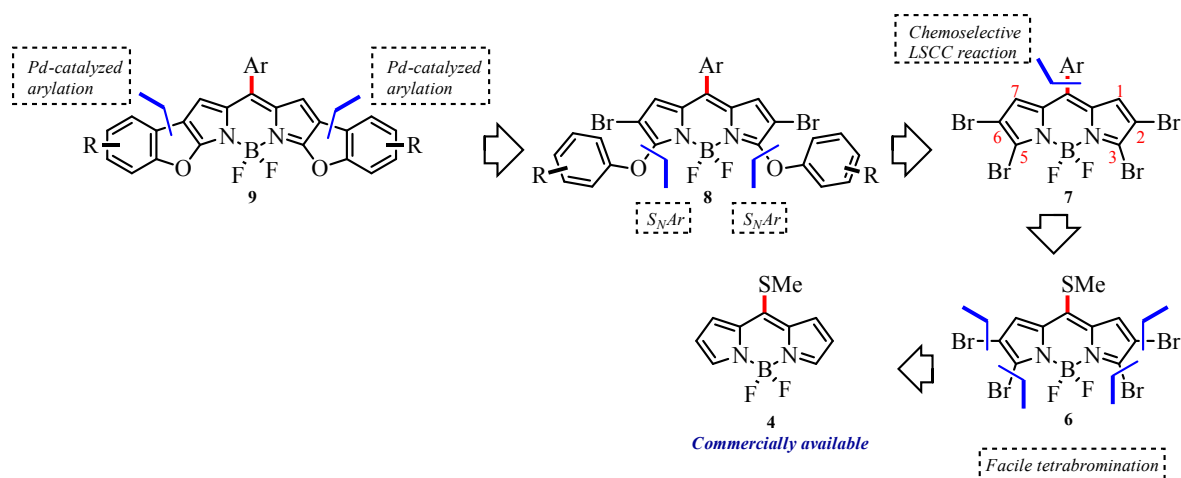
Herein we disclose a fully flexible method that allows the preparation of a novel family of benzofuran-fused BODIPY dyes. Easy modifications in the synthesis permits variations both at the *meso*-position and the benzofuran substitution pattern since the latter only requires substituted phenols. This method also features the use of an advanced, commercially available BODIPY starting material **4**, a complete chemoselective control over three reaction sites, and the preparation of BODIPY dyes with unique architectures and important photophysical and laser properties. In 2016,<sup>33</sup> we reported the synthesis of multifunctional BODIPY **5** and demonstrated that it displayed orthogonal reactivity, i.e., the C-S bond was activated under the Liebeskind-Srogl cross-coupling reaction (LSCC)<sup>34</sup> conditions, leaving the C-Br bond intact. This chemoselectivity allowed us to introduce a variety of functional groups in a programmed fashion on the periphery of the BODIPY core. Now we decided challenge even further the chemoselectivity of novel BODIPY building block **6** and apply it this time to the preparation of a new family of benzofuran-fused BODIPY dyes (Figure 3).

**Previous work:****This work:****Figure 3.** BODIPY dyes with orthogonal reactivity.

This type of benzofuran-fused BODIPYs readily available by this novel approach, display well red-shifted absorption and emission bands. Hereafter, we describe the photophysical and lasing properties of the benzofuran-fused BODIPYs and demonstrate their viability as laser dyes endowed with high laser and fluorescence efficiencies, and high photostability under strong and prolonged pumping. To the best of our knowledge, the laser capabilities of the red-emitting benzo-fused BODIPYs overall are almost hitherto unexploited (just early conference proceedings from SPIE).<sup>35</sup>

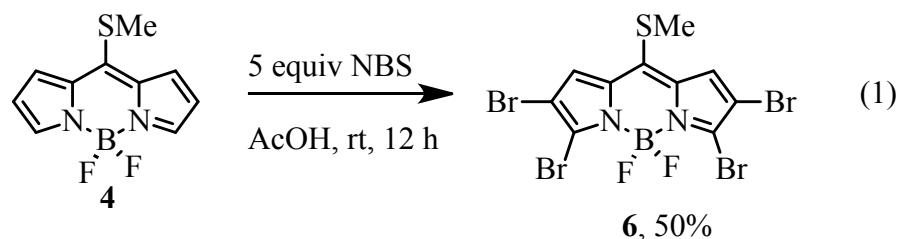
## Results and Discussion

**Retrosynthetic analysis.** The retrosynthetic analysis is shown in Scheme 3. The final products **9** will be formed after a Pd-catalyzed arylation reaction of **8**.<sup>36</sup> Bis-phenoxy-containing intermediate **8** would be formed after a double  $S_NAr$  of **7** with substituted phenols under basic conditions, at exclusively at the 3- and 5-positions since only those C-Br bonds are activated towards the addition-elimination process.<sup>37</sup> *Meso*-aryl substituted BODIPY **7** would be prepared from the chemoselective LSCC under neutral conditions leaving intact the four brominated positions.<sup>33</sup> This selectivity would allow for the introduction of varied aryl groups at the *meso*-position, a key step of our synthetic plan. Finally, tetrabrominated intermediate **6** would be produced from commercially available **4**.



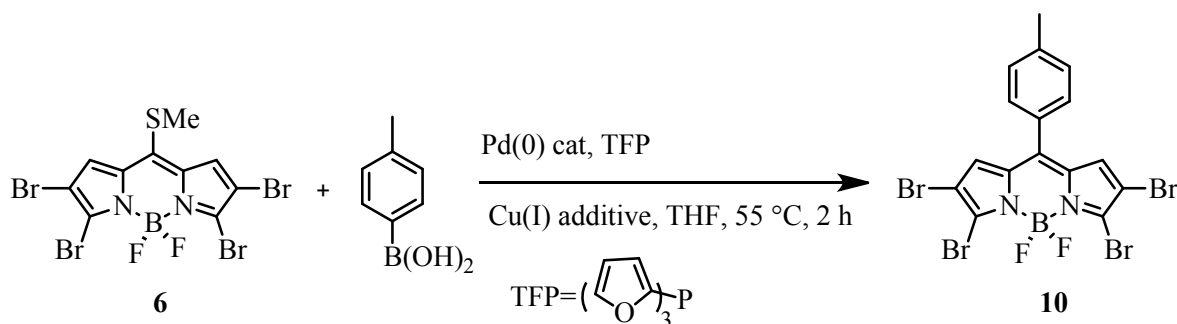
### Scheme 3. Retrosynthetic analysis to prepare benzofuran-fused BODIPY dyes

**Synthesis.** Tetrabromination of commercially available 8-methylthioBODIPY **4** was carried out according to eq 1.



Next, the key step of our synthetic plan followed, i.e., the chemoselective LSCC on **6** in the presence of other reactive sites (Table 1).

**Table 1. Optimization of the LSCC reaction on 6.<sup>a</sup>**



Entry	Equiv boronic acid	Cu source	Pd source	% of conversion <sup>b</sup>
1	1	CuTC <sup>c</sup>	Pd <sub>2</sub> (dba) <sub>3</sub>	72
2	3	CuTC	Pd <sub>2</sub> (dba) <sub>3</sub>	80
3	3	CuMeSal <sup>d</sup>	Pd <sub>2</sub> (dba) <sub>3</sub>	24
4	3	CuO <sub>2</sub> PPh <sub>2</sub> <sup>e</sup>	Pd <sub>2</sub> (dba) <sub>3</sub>	65
5	3	CuI	Pd <sub>2</sub> (dba) <sub>3</sub>	- <sup>f</sup>
6	3	CuTC	Pd(PPh <sub>3</sub> ) <sub>4</sub> <sup>g</sup>	10

<sup>a</sup>Conditions: **6** (1 equiv), Pd(0) (2.5 mol%), TFP (2.5 mol%), Cu(I) source (equimolar with respect to the boronic acid). <sup>b</sup>Determined by HPLC. <sup>c</sup>Copper(I) thiophene-2-carboxylate.

<sup>d</sup>Copper(I) 3-methylsalicylate. <sup>e</sup>Copper(I) diphenylphosphinate. <sup>f</sup>No product was formed.

<sup>g</sup>No TFP was used.

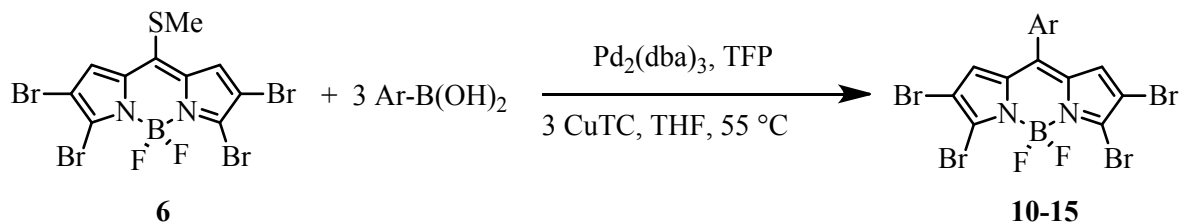
The typical Cu(I) sources for the LSCC reaction were tested. All of them, except CuI yielded the desired product (entry 5), however, the best results were observed with CuTC (entry 1).

A further increase in the yield was observed when 3 equiv of the boronic acid were used (entry 2). Notably, under these reaction conditions, only BODIPY **10** was produced along with trace amounts of other colored compounds in quantities too small to be characterized.

This key result allowed the selective functionalization of the *meso*-position leaving the other brominated positions available to be manipulated at will.

Once the best conditions were determined, we set out to react **6** with several arylboronic acids (Table 2) to study the scope of the LSCC reaction.

**Table 2. LSCC reaction on BODIPY **6**.**<sup>a</sup>



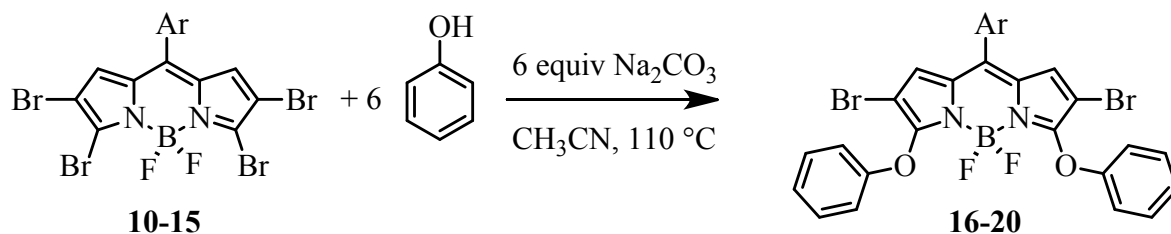
Entry	Ar-	Reaction time	% Yield <sup>b</sup>	Compound
1		2 h	50	<b>10</b>
2		1 h	76	<b>11</b>
3		1 h	38	<b>12</b>
4		40 min	63	<b>13</b>
5		2h	18	<b>14</b>
6		1 h	83	<b>15</b>

<sup>a</sup>Conditions: **6** (1 equiv), boronic acid (3 equiv), Pd<sub>2</sub>(dba)<sub>3</sub> (2.5 mol%), TFP (2.5%), CuTC (3 equiv), in THF at 55 °C. <sup>b</sup>Isolated yield.

The LSCC took place smoothly in the set of phenols that we studied to give the *meso*-aryl-substituted products in modest to good yields in relatively short reaction times. Electron-rich boronic acids gave the highest yields (entries 4 and 6). No detrimental effect due to sterics

was observed when *o*-tolylboronic acid was employed (entry 2). Once derivatives **10-15** were obtained, the nucleophilic substitution of phenol at the 3-position was explored. The results are given in Table 3.

**Table 3. Nucleophilic substitution of phenol on derivatives 10-15.<sup>a</sup>**



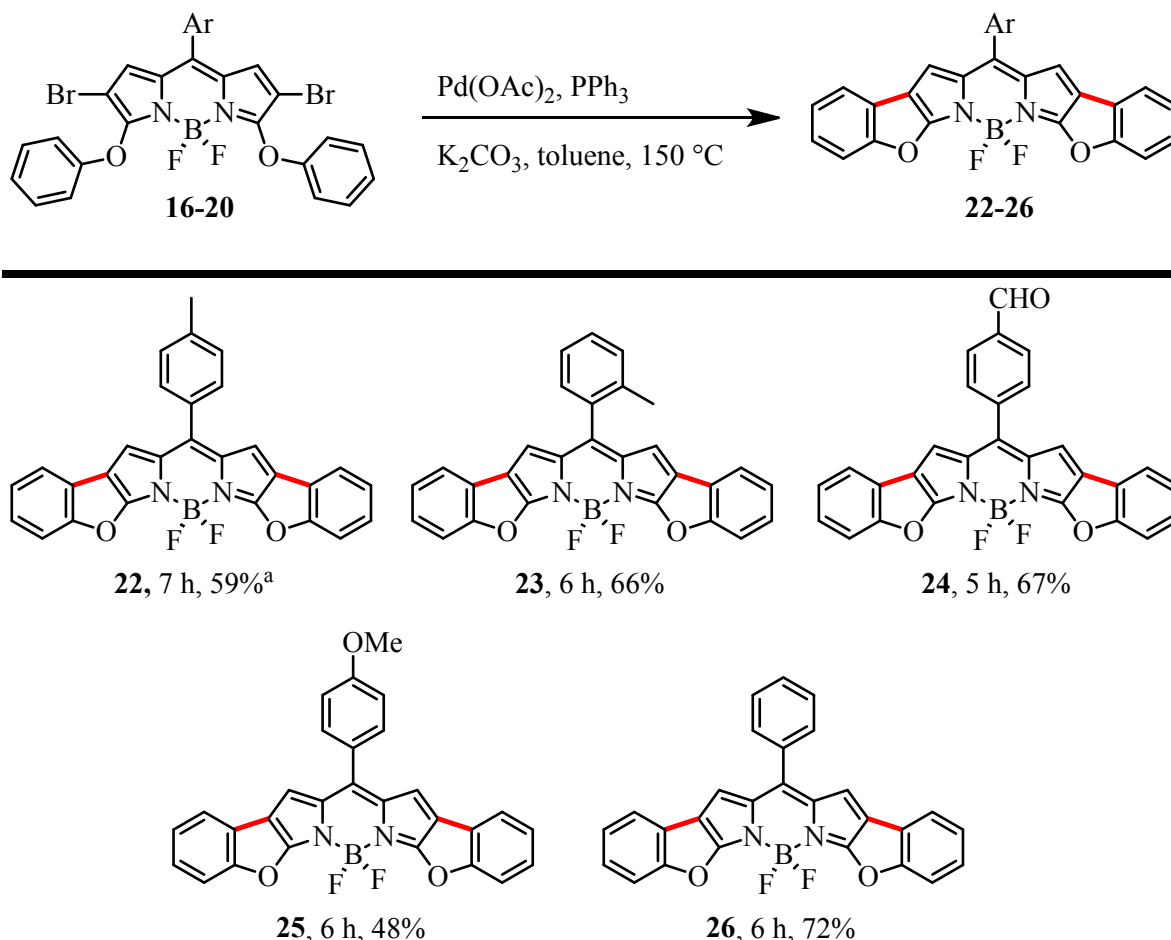
Entry	Ar	Reaction time (h)	% Yield <sup>b</sup>	Compound
1		6	80	<b>16</b>
2		3	77	<b>17</b>
3		3	57	<b>18</b>
4		5	72	<b>19</b>
5		3	60	<b>20</b>
6		-	- <sup>c</sup>	<b>21</b>

<sup>a</sup>Conditions: BODIPYs (1 equiv), phenol (6 equiv), Na<sub>2</sub>CO<sub>3</sub> (6 equiv), sealed tube.

<sup>b</sup>Isolated yields. <sup>c</sup>Decomposition of the BODIPY was observed.

Phenol was added to BODIPYs **10-15** under basic conditions in acetonitrile at 110 °C.<sup>32</sup> The two-fold substitution reaction took place uneventfully to give 3,5-diphenoxy-substituted BODIPY dyes in good yields (entries 1-5). However, when trying to add phenol to BODIPY **15**, decomposition of this compound was observed.

Next, the polyfunctionalized BODIPY so prepared were subjected to the Pd-catalyzed intramolecular arylation (Chart 1).

**Chart 1. Pd-catalyzed arylation of BODIPYs 16-20.<sup>a,b</sup>**

<sup>a</sup>Conditions: BODIPY (1 equiv), Pd(OAc)<sub>2</sub> (0.05 equiv), PPh<sub>3</sub> (0.1 equiv), K<sub>2</sub>CO<sub>3</sub> (3 equiv), in toluene at 150 °C in a sealed tube. <sup>b</sup>Isolated yield.

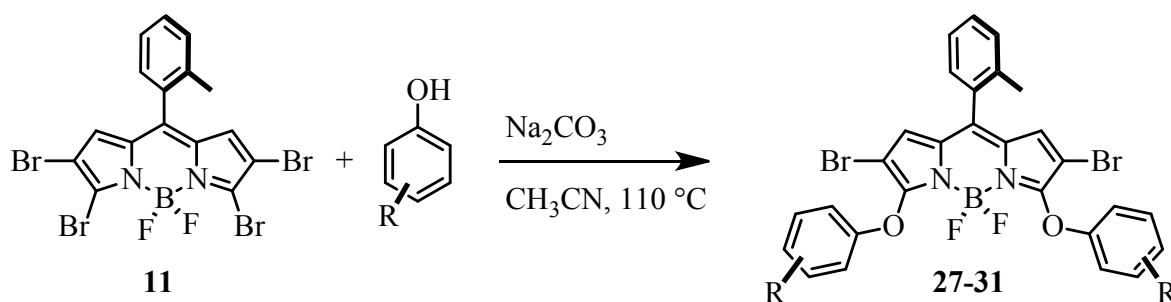
In sharp contrast to the reaction conditions that gave rise to isomer **3**,<sup>38</sup> two-fold arylation reaction of dyes **16-20** was achieved under mild conditions to furnish the cyclized products in yields that ranged from 48% to 72%. The electronic properties of the *meso*-aryl ring did not seem to have any significant influence in either the reaction time, or the resulting isolated yield.

We then decided to study the scope and limitations of the overall process using various substituted phenols (Table 4). Compound **11** was chosen to start the sequence because it has hindered rotation around the C<sub>meso</sub>-aryl bond. This feature increases the probability of

observing a high fluorescent quantum yield ( $\Phi_{fl}$ ) in the final products due to restricted rotation of said bond, thereby inhibiting non-radiative relaxation pathways.<sup>39</sup>

**Table 4. Addition-elimination reaction of substituted phenols on tetrabromoBODIPY**

11.<sup>a</sup>



Entry	Phenol derivative	Reaction time	% Yield <sup>b</sup>	Compound
1		2 h	79	27
2		2 h	90	28
3		1 h	90	29
4		1 h	81	30
5		2h	58	31
6		2.5 h	- <sup>c</sup>	32
7		15 min	- <sup>d</sup>	33

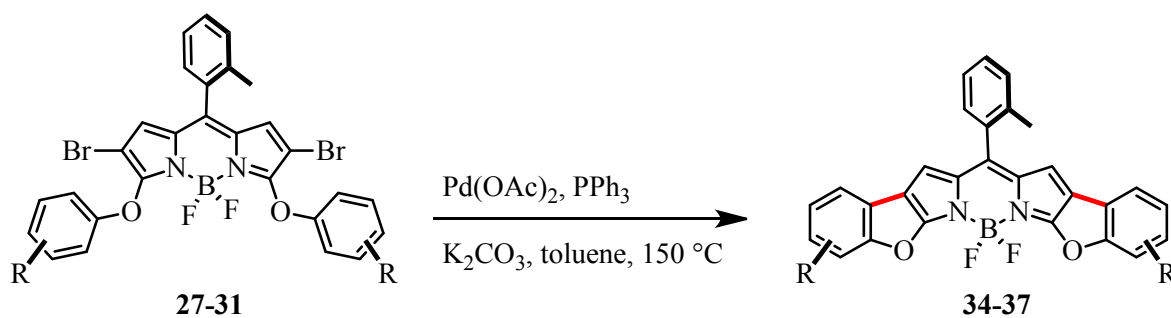
<sup>a</sup>Conditions: BODIPY (1 equiv), phenol (6 equiv), Na<sub>2</sub>CO<sub>3</sub> (6 equiv), in MeCN at 110 °C in a sealed tube. <sup>b</sup>Isolated yields. <sup>c</sup>The product decomposed on chromatography (SiO<sub>2</sub>-gel) purification. <sup>d</sup>Decomposition was observed.

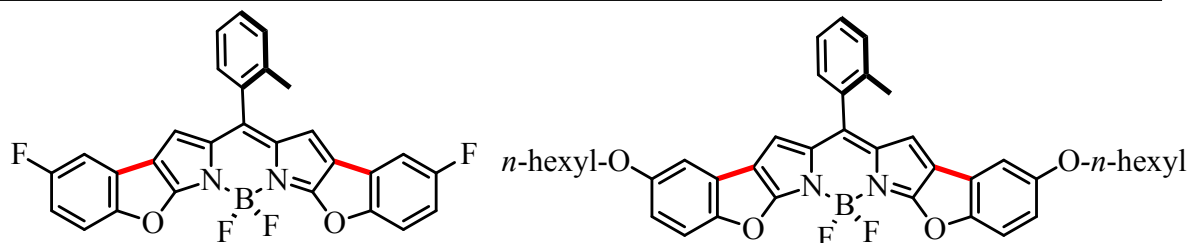
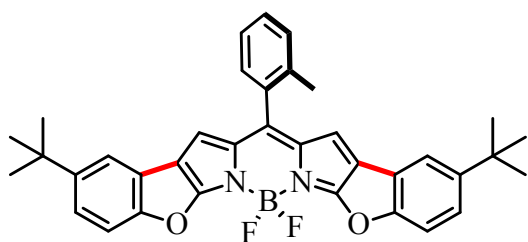
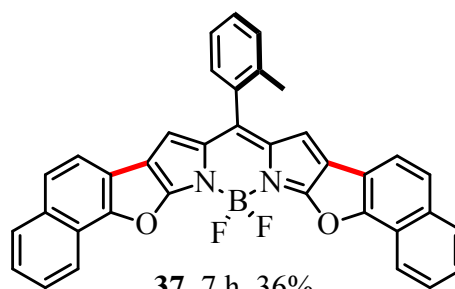
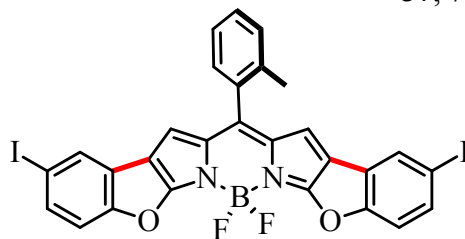
Addition of substituted phenols took place as expected. All the products were obtained, except when 4-hydroxyphenylpinacol boronate, and 1-hydroxypyrene were used, for decomposition was observed in both cases (entries 6 and 7). Addition of the rest of the

1  
2  
3 substituted phenols and naphthol was carried out under mild reaction conditions and short  
4 reaction times (1-2 h) to yield the highly colored products in good to excellent yields (entries  
5  
6  
7  
8 1-5).

9  
10 With derivatives **27-31** in hand, we proceeded to study their Pd(0)-catalyzed ring-closure to  
11  
12 yield the corresponding benzofuran-fused products. The results are illustrated in Chart 2.  
13  
14

15  
16  
17 **Chart 2. Pd-catalyzed arylation of BODIPYs 27-31.**<sup>a,b</sup>  
18



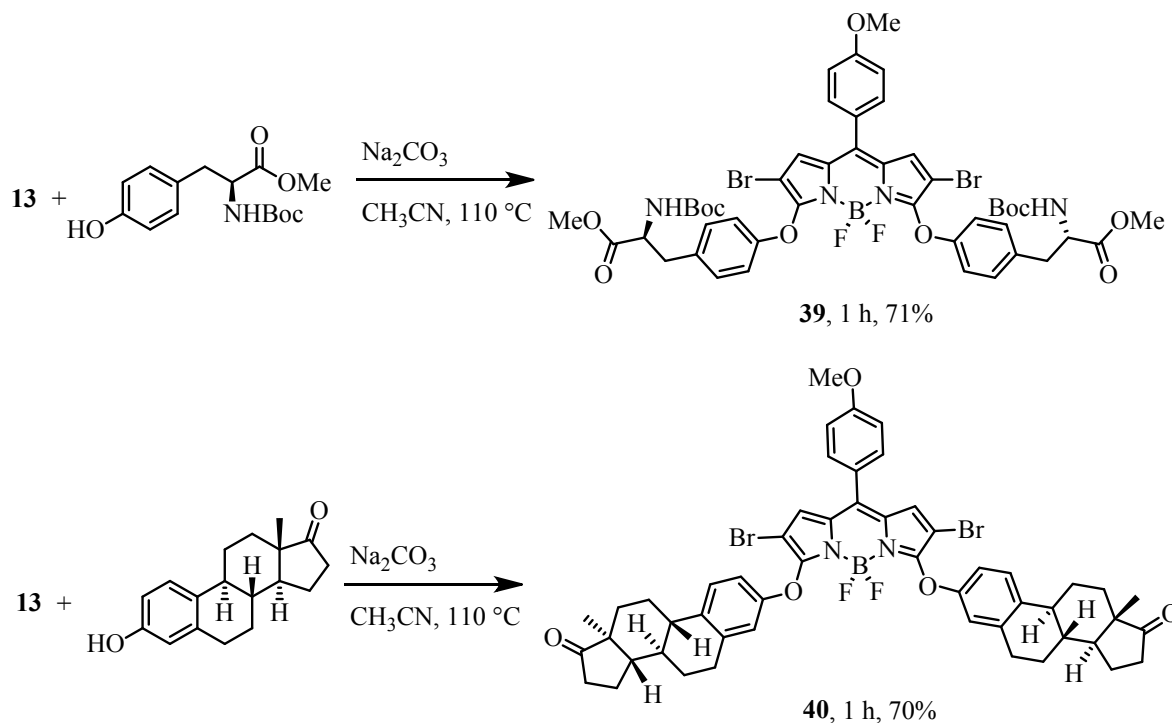
**34**, 6 h, 75%**35**, 7 h, 69%**36**, 6 h, 64%**37**, 7 h, 36%**38**, 30 min, -

<sup>a</sup>Conditions: BODIPY (1 equiv), Pd(OAc)<sub>2</sub> (0.05 equiv), PPh<sub>3</sub> (0.1 equiv), K<sub>2</sub>CO<sub>3</sub> (3 equiv), in toluene at 150 °C in a sealed tube. <sup>b</sup>Isolated yields.

Satisfyingly, the cyclization reaction took place to produce the final products in moderate to good yields. Iodine-containing derivative **38** was not formed since quick decomposition of the starting material was observed within the first 30 min. Presumably, the more reactive iodide participated in undesired reaction in the presence of Pd.

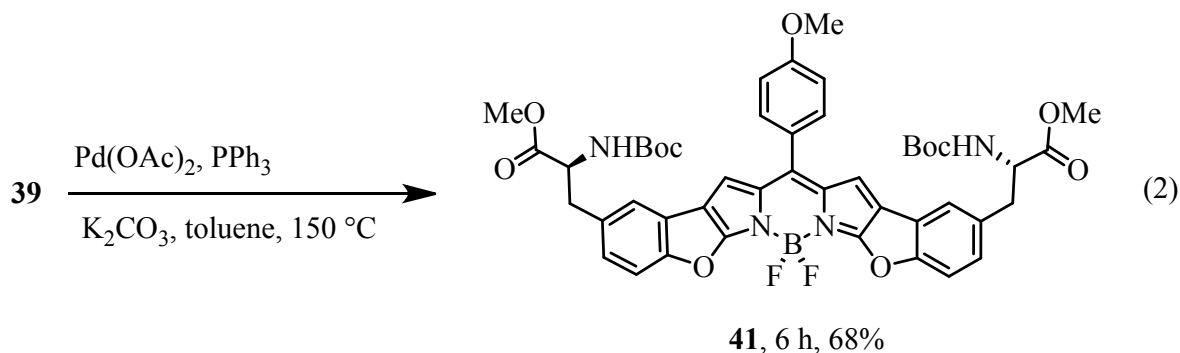
**Incorporation of two biomolecules.** To demonstrate the applicability of the methodology described herein, two phenolic biomolecules were chosen to be incorporated to the BODIPY core: estrone and *N*-BOC-*L*-tyrosine methyl ester. TetrabromoBODIPY **13** was chosen as the starting material since the *o*-tolyl analogue **11** would give rise to diastereoisomeric final

products due to its hindered rotation around the *meso*-sigma bond. To this end, both biomolecules were reacted with **13** under the reaction conditions shown in Tables 3 and 4 (Scheme 4) yielding the expected products in good yields and short reaction times.



#### Scheme 4. Reaction of estrone and *N*-BOC-*L*-tyrosine methyl ester with BODIPY **13**.

We then proceeded to carry out the arylation reaction on both **39** and **40** that would produce the final products according to the conditions depicted in Charts 1 and 2. Cyclization of **39** gave the fused derivative **41** in 68% yield after 6 h (eq 2).



Cyclization of **40** posed an interesting regiochemistry issue since the estrone fragment has two nonequivalent reaction sites (Figure 4).

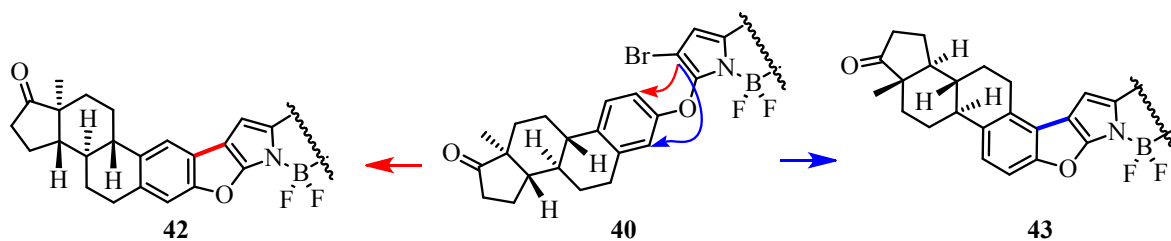
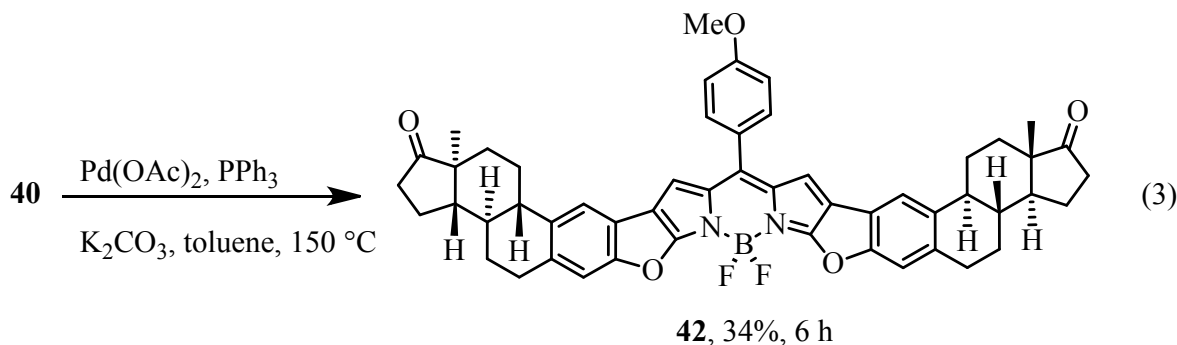


**Figure 4.** The two possible regioisomers that could be produced from the cyclization reaction of **40**.

Bearing these aspects in mind, the Pd-catalyzed arylation reaction on BODIPY **40** was carried out (eq 3). Even though the overall isolated yield was low (34%), only regioisomer **42** was obtained after 6 h.



Inspection of the NMR data led us to this conclusion. If isomer **43** had been formed, in addition to the characteristic AA'XX' coupling pattern of the 8-(*p*-MeOphenyl) fragment, and a singlet of the pyrrole moiety, two doublets should appear in the aromatic region due to the *cis*-hydrogens from the estrone fragment (red protons in Figure 5). On the other hand, if **42** was formed, the two aromatic protons of estrone would be *para*- to each other (blue protons in Figure 5), and therefore uncoupled. Indeed, the latter is the pattern we observe.

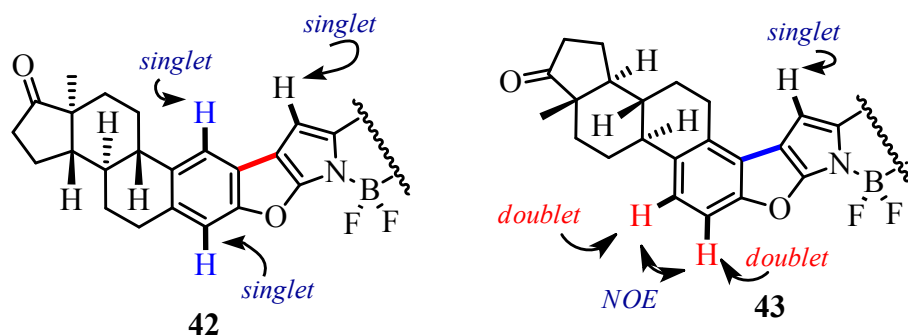


**Figure 5.** Expected  $^1\text{H}$  NMR signals of isomers **42** and **43**.

The actual COSY spectrum of **42** is illustrated in Figure 6, showing no cross-peaks between aromatic protons d and e.

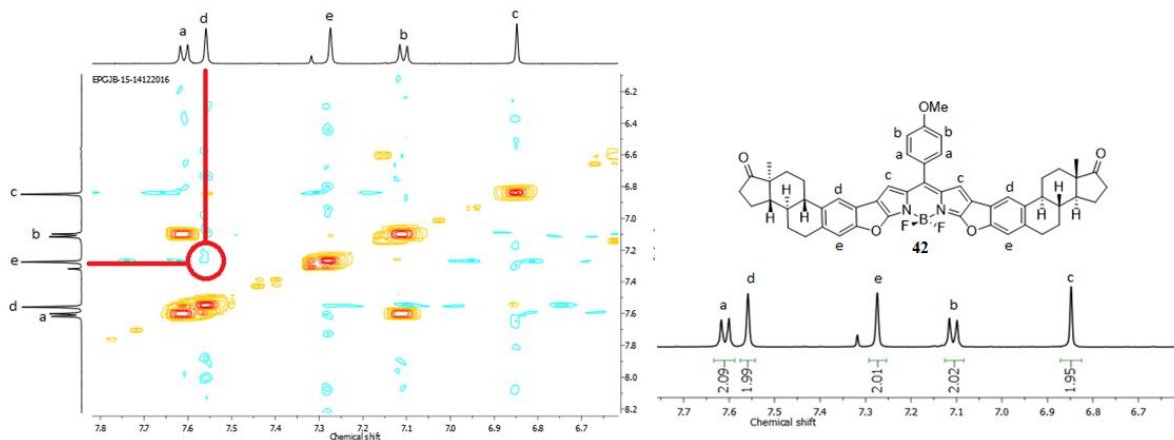
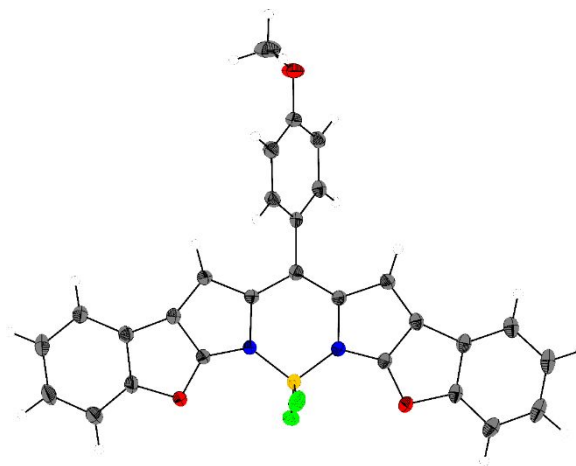


**Figure 6.** Aromatic region of the COSY spectrum of estrone-fused BODIPY **42**.

**X-ray structure of 25.** BODIPY **25** was crystallized by diffusion from petroleum ether/ $\text{CH}_2\text{Cl}_2$  (Figure 7). The heterocyclic fragment of **25** is almost planar, displaying a very slight concavity at the center. On the other hand, the B atom has a tetrahedral geometry (the F-B-F angle is  $110^\circ$ , and the N-B-N angle is  $104^\circ$ ) and lies off the plane by  $10^\circ$ . The 8-aryl ring is in a  $55^\circ$  angle with respect to the BODIPY plane owing to the steric hindrance between the hydrogens placed at *ortho* position of the ring and those at the chromophoric positions 1

1  
2  
3 and 7. The X-ray structure of the tolyl analogue **22**, was already reported and displays very  
4  
5 similar features.<sup>32</sup>  
6

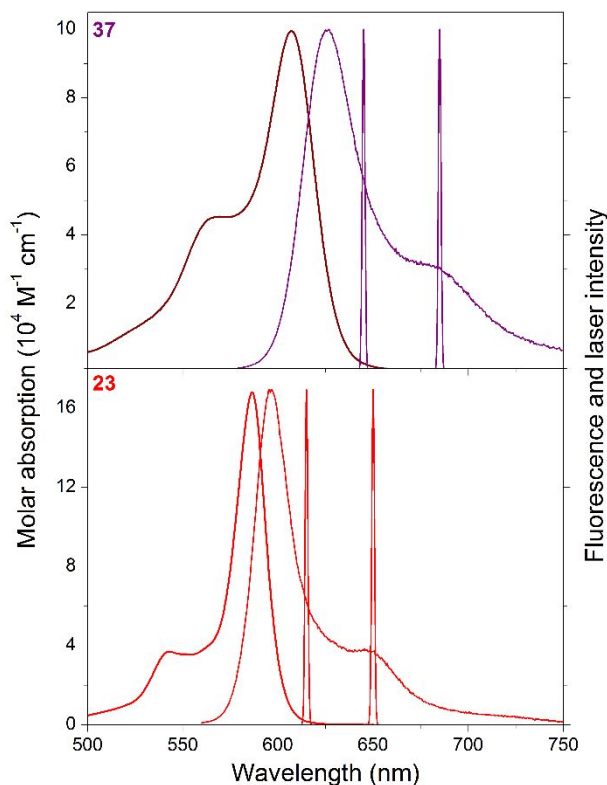


7  
8  
9  
10  
11  
12  
13  
14  
15  
16  
17  
18  
19  
20  
21  
22  
23  
24 **Figure 7.** X-ray structure of **25** (ORTEP drawing, 50% probability). The corresponding  
25  
26 crystallographic data are listed in Table S3.  
27  
28  
29

### 30 31 **Photophysical properties**

32  
33  
34 The fusion of benzofuran rings to the  $\alpha$ - $\beta$  positions of the dipyrrole core extends the  $\pi$ -system  
35  
36 and, in turn, entails a pronounced bathochromic spectral shift that pushes the spectral band  
37  
38 towards the red spectral window (Figure 8 and S1-S3). In contrast, the *meso*-aryl group has  
39  
40 no effect in the spectral band positions. In fact, in the compounds bearing methyl at *ortho*  
41  
42 position of the 8-phenyl, the sterical hindrance places this ring almost orthogonal to the  
43  
44 dipyrrole plane (dye **23**). But even in absence of such alkylation (dye **22** or **26** for example in  
45  
46 Chart 1) the 8-phenyl is also twisted (around  $60^\circ$ ), owing to steric hindrance with the  
47  
48 hydrogens at chromophoric positions 1 and 7, and, hence, it is not electronically coupled to  
49  
50 the chromophoric core. Such red shift is strengthened by the addition of larger and more  
51  
52 conjugated aryls groups to the chromophoric core. For instance, in dye **37**, with an aromatic  
53  
54  
55  
56  
57  
58  
59  
60

1  
2  
3 framework comprising up to seven aromatic rings, the spectral bands are located well above  
4 600 nm (Figure 8). The electrochemistry measurements reveal that all the dyes have a similar  
5 cyclic voltammogram featuring two well-resolved and reversible anodic (around 1.25 V) and  
6 cathodic (around -0.75 V) waves (Figure 9 and S4). The extension of the chromophoric  
7 framework (dye **37**) implies a reduction of both redox potential (with regard to its analog **23**,  
8 Figure 9), in agreement with the calculated lower energy gap between the frontier molecular  
9 orbitals (from 5.80 eV in **23** to 5.73 eV in **37**) and the recorded bathochromic shift (Figure  
10 8).  
11  
12  
13  
14  
15  
16  
17  
18  
19  
20  
21  
22  
23



48 **Figure 8.** Absorption, normalized fluorescence, and laser (dual emission depending on the  
49 dye concentration) spectra of dye **23** and its analogue **37**, with additional fused phenyl rings,  
50 in ethyl acetate. The spectra of the rest of compounds are included in Figure S1-S3.  
51  
52  
53  
54  
55  
56  
57  
58  
59  
60

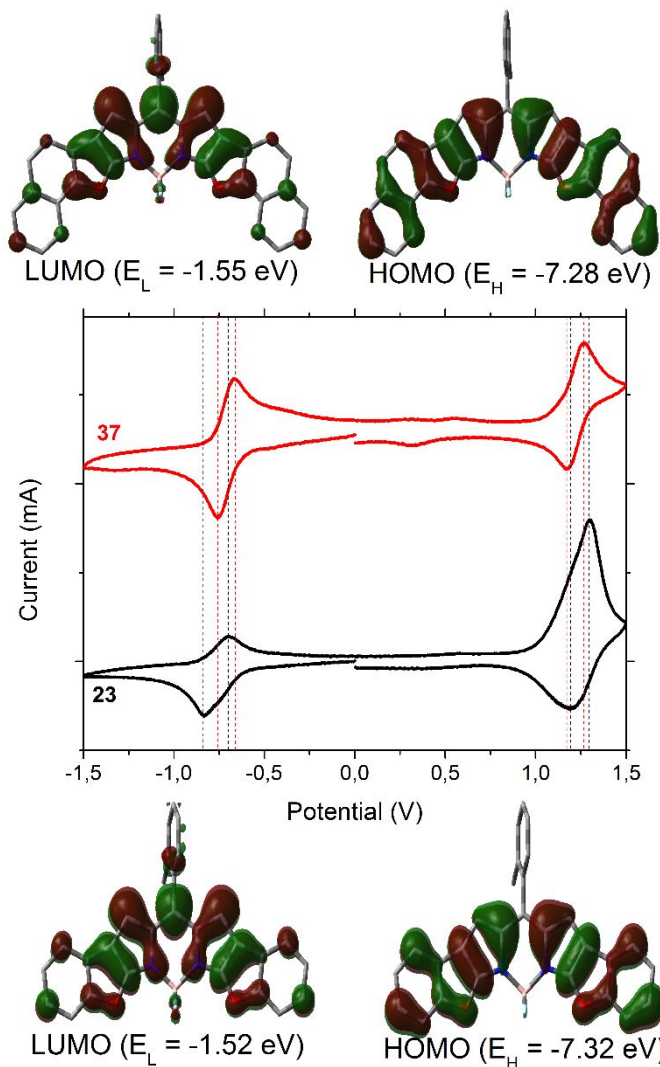


**Figure 9.** Cyclic voltammograms and calculated contour maps and energies of the frontier orbitals for compounds **23** and **37**. Additional voltammograms of representative compounds are collected in Figure S4.

Despite the number of rings fused to the dipyrin core, and the ensuing structural stress, the whole chromophore remains planar (for instance, deviations lower than  $2^\circ$  in compound **26**, even in the excited state). As a result of this planar and rigid molecular structure, reflected in a low Stokes shift (overall lower than  $500\text{ cm}^{-1}$ , Table S1), the aromaticity is high (as testified by Bonds Length Alternation, BLA, parameter around 0.02 in both ground and excited state). These features explain the remarkable high absorption probability (reaching values higher

than  $2 \cdot 10^5 \text{ M}^{-1} \text{ cm}^{-1}$ , Table 5), notable radiative rate constant ( $k_{\text{fl}} > 2 \cdot 10^8 \text{ s}^{-1}$ , Table 5) and low internal conversion probability (Table 5). Therefore, these conformationally restricted and symmetrical red-emitting dyes display a bright fluorescence response, approaching a 100% in apolar media (Table 5). It should be highlighted that the presence of unconstrained 8-aryl fragments with conformational freedom, efficiently quenches the fluorescence response in simpler and more compact BODIPYs.<sup>40</sup> In contrast, in the herein tested dyes, the extension of the  $\pi$ -system through the aryls fused to the pyrroles, shifts the electronic density away from the key *meso* position, avoiding, or at least hampering, the quenching pathway associated to the 8-aryl motion.<sup>33</sup> In fact, those dyes sharing the same chromophoric unit (dipyrrin fused with benzofurans), but differing in the *meso*-substitution, show similar and high fluorescence quantum yields (Table 5) regardless of the conformational mobility of the 8-aryl (unconstrained, twisting angle of the phenyl around  $65^\circ$  in dyes **22** and **26**, or constrained, orthogonal *ortho*-tolyl in **23**) or its functionalization (electron donor *para*-methoxy in **25**). The only exception to the rule is **24** with a *para*-formylated 8-aryl, which shows an unexpected low fluorescence response (Table 5). Such exemption will be rationalized below.

**Table 5.** Photophysical properties of red-emitting benzofuran-fused BODIPYs in cyclohexane. The whole photophysical data in more solvents are listed in Table S1.

	$\lambda_{\text{ab}}$ (nm)	$\epsilon_{\text{max}}$ ( $10^4 \text{ M}^{-1} \cdot \text{cm}^{-1}$ )	$\lambda_{\text{fl}}$ (nm)	$\Delta\nu_{\text{St}}$ ( $\text{cm}^{-1}$ )	$\phi$	$\tau$ (ns)	$k_{\text{fl}}$ ( $10^8 \text{ s}^{-1}$ )	$k_{\text{nr}}$ ( $10^8 \text{ s}^{-1}$ )
<b>22</b>	548.5	21.5	596.5	345	0.88	4.09	2.15	0.29
<b>23</b>	586.5	21.5	595.5	260	0.88	4.21	2.09	0.29
<b>24</b>	592.5	13.7	612.0	540	0.63	2.47	2.55	1.49
<b>25</b>	583.5	20.0	593.5	290	0.88	4.10	2.14	0.29
<b>26</b>	586.0	15.6	597.5	330	0.84	3.99	2.10	0.40
<b>34</b>	581.5	17.3	590.0	250	0.95	4.02	2.35	0.14

<b>35</b>	592.0	19.0	603.0	310	0.96	4.12	2.33	0.09
<b>36</b>	591.5	23.2	602.0	295	0.89	4.11	2.16	0.27
<b>37</b>	613.0	12.9	625.0	315	0.81	4.31	1.89	0.43
<b>41</b>	586.5	18.0	596.5	285	0.81	3.94	2.07	0.47
<b>42<sup>a</sup></b>	596.5	17.9	611.5	410	0.88	4.04	2.18	0.30

<sup>a</sup>**42** was insoluble in cyclohexane, thus, the reported data were recorded in diethylether

The evolution of the fluorescence efficiency with the solvent depends both on the type of functional groups decorating the chromophoric backbone, and on the number of fused rings (Figure 10 and Table S1). Thus, the presence of heteroatoms, like fluorine **34**, or alkyl groups (bulky *tert*-butyl in **36**) or a functionalized aliphatic chain (tyrosine biomolecule in **41**) in the fused benzofuran, renders highly fluorescent dyes in all the considered solvents. In contrast, the addition of alkoxy chains (**35**) induces a progressive decrease of both the fluorescence efficiency and the fluorescence lifetime with the solvent polarity (down to 29% and 1.67 ns, respectively, in methanol, Table S1). Such tendency is consistent with the activation of an intramolecular charge transfer (ICT) state in polar media. Thus, the benzofuran itself could act as an electron donor owing to its oxygen heteroatom at the  $\alpha$ -pyrrolic position. The additional presence of alkoxy groups in the periphery increases such electron donor character, thereby being high enough as to switch on the non-fluorescence ICT. Indeed, in the contour maps depicted in Figure 9, it can be visualized some electron transfer from the benzofuran to the dipyrin upon excitation (from HOMO to LUMO). Likely, such charge separation is enlarged with fused benzofuran bearing alkoxy moieties, further favoring the non-radiative energy loss through the claimed ICT. Moreover, similar red-emitting dyes have been reported in the literature but with nitrogen instead of oxygen (fusion of indole).<sup>41</sup> The higher electron donor ability of the aza group induced a more pronounced spectral red shift but lower fluorescence efficiencies than the herein tested analog **26**, likely related to a higher charge

1  
2  
3 transfer probability. In this line of reasoning, the presence of electron withdrawing groups at  
4 the 8-aryl moiety, albeit moderately weak like the formyl group in dye **24**, could reinforce  
5 the formation of ICT processes, owing to the induced push-pull character (from the alkoxy-  
6 containing benzofuran to the formylated 8-phenyl group), explaining the above-mentioned  
7 unexpected quenching of this dye in polar media (Figure 10 and Table 5). To unambiguously  
8 back up the ongoing ICT as the key process which rules the fluorescence response in these  
9 last dyes (**24** and **35**), we have measured the photophysical properties of the structurally  
10 related analogs **22** (bearing a non-formylated 8-phenyl ring) and **24** (with the said formylated  
11 ring) in a battery of solvents with different physicochemical properties (Table S2). Whereas  
12 in the former dye **22** the fluorescence quantum yield remains high (always higher than 0.84,  
13 Table S2 and Figure S5) regardless of the solvent properties (described by the normalized  
14  $E_T(30)$  solvent scale<sup>42</sup>), in the last dye **24** not only the fluorescence quantum yields are lower,  
15 but also the values show a marked dependency on the solvent polarity (from 0.63 in  
16 cyclohexane down to 0.37 in acetonitrile, Table S2 and Figure S5). Such decrease of the  
17 fluorescence efficiency with the solvent polarity is a fingerprint of an ongoing dark ICT,  
18 which quenches the emission from the locally excited (LE) state, mainly in polar media where  
19 the low-lying ICT is further stabilized. Indeed, the recorded fluorescence quantum yield for  
20 dye **24** in a polar/protic solvent (methanol) does not follow the expected trend (Figure S5)  
21 and the value is higher (0.44, Table S2). Such exception is likely due to a specific interaction  
22 with the electron donor (oxygen atom of the benzofuran) which hampers the population of  
23 the photoinduced ICT state.  
24  
25  
26  
27  
28  
29  
30  
31  
32  
33  
34  
35  
36  
37  
38  
39  
40  
41  
42  
43  
44  
45  
46  
47  
48  
49  
50  
51  
52  
53  
54  
55  
56  
57  
58  
59  
60

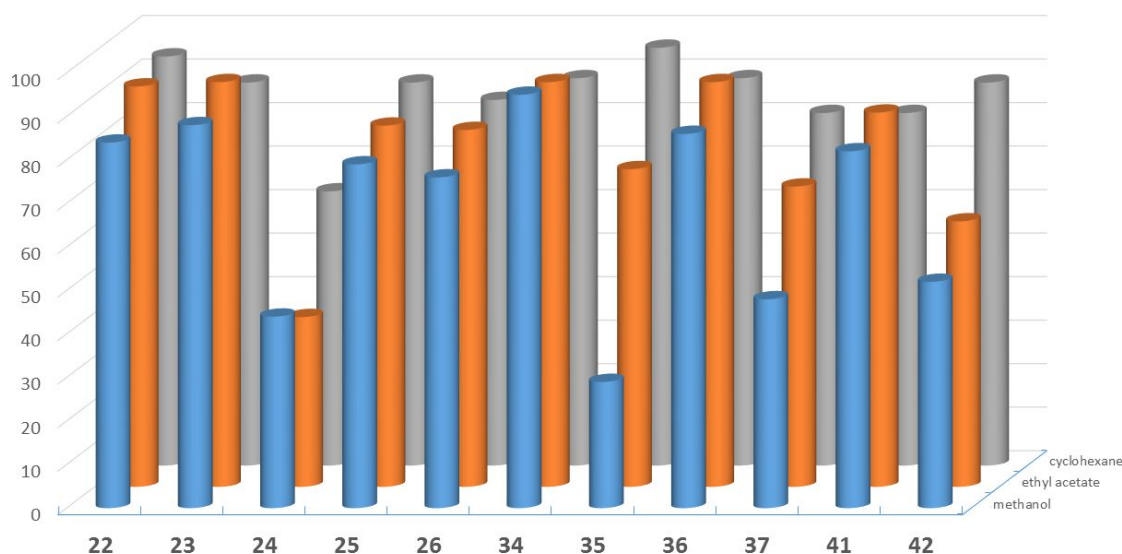


**Figure 10.** Evolution of the fluorescence quantum yield of the herein reported novel red-emitting BODIPYs with the tested media (from apolar cyclohexane in grey to polar methanol in blue).

On the other hand, compounds **37** and **42**, bearing the highest number of fused aryl fragments, show low fluorescence efficiencies in polar media (down to 50% in methanol, Figure 10), albeit the fluorescence lifetimes remain similar (around 3 ns) (Table 5). In these highly extended derivatives, the structural stress to keep the whole chromophore planar should be high, although theoretical calculations predict that the chromophore remains quite planar. However, in the more polar media, where the interactions are stronger, such planarity could be slightly distorted, likely increasing the internal conversion relaxation with the consequent reduction in the fluorescence ability. Alternatively, a further addition of aromatic rings to the chromophoric core could increase the charge separation, enhancing the non-radiative deactivation pathways in polar media.

## Laser Properties

In view of the high fluorescence efficiency of these red-emitting dyes, we tested their performance as active media for tunable lasers (see methods in ESI). Owing to the limited solubility of some of the dyes in apolar media, we chose ethyl acetate as the right solvent to measure the laser properties. In addition, this solvent allows assessing the prospects of doping these dyes into solid-state dye lasers (SSDL), as it mimics the chemical structure of methyl methacrylic polymers.<sup>43</sup> Hence, the laser characterization and optimization in ethyl acetate could be directly extrapolated to these polymers. Even so, in the most functionalized and largest dyes the solubility was restricted to 0.5 mM (**37** and **41**) or the required concentration to attain laser emission could not be reached (**42**).

**Table 6.** Laser properties of red-emitting benzofuran-fused BODIPYs in ethyl acetate at the optimum dye concentration. The full set of laser data as a function of dye concentration are listed in Table S3. The data corresponding to the commercially available red-emitting BODIPY laser dye (PM650) are included for comparison.

Dye	[Dye] (mM)	Eff <sup>a</sup> (%)	$\lambda_{\text{peak}}$ (nm)	$E_{\text{dose}}^{90\%}$ (GJ/mol)
<b>22</b>	0.75	44	646.5	2.14
<b>23</b>	0.50	48	648.8	3.30
<b>24</b>	0.50	28	636.0	1.07
<b>25</b>	1.00	45	645.2	0.96
<b>26</b>	0.75	44	647.2	1.94
<b>34</b>	1.25	43	642.0	7.39
<b>35</b>	1.25	43	657.6	5.26
<b>36</b>	0.75	43	656.2	4.24
<b>37</b>	0.50	27	685.0	4.46
<b>41</b>	0.50	40	650.0	1.96
<i>PM650</i>	<i>1.00</i>	<i>31</i>	<i>656.5</i>	<i>6.29</i>

<sup>a</sup>Eff: Laser efficiency or ratio of output/input energy;  $\lambda_{\text{peak}}$ : Laser peak wavelength;  $E_{\text{dose}}^{90\%}$ : Molar energy dose needed to reduce LIF to a 90% of its initial value (see methods for a detail description).

1  
2  
3 The laser properties correlate, *grosso modo*, with the photophysical signatures (Table 5 and  
4 S1). At high concentrations, all the dyes (with the aforementioned exception of **42** owing to  
5 solubility reasons) display a laser emission line far away from the absorption and  
6 fluorescence band (around 70 and 50 nm, respectively), much stronger than what is usually  
7 recorded for BODIPY dyes (around 40 and 20 nm, respectively).<sup>44</sup> In particular, dye **37**  
8 presents the redder laser band, which is centered at 685 nm thanks to its higher number of  
9 aromatic rings fused to the chromophoric core (Figure 8). In contrast, at low concentrations  
10 or low pump energies, the laser emission band appears in the expected position for BODIPYs  
11 (Figure 8), leading, in some cases, to bichromatic emission (Figure 11 and Table S3). Such  
12 dual laser emission has been previously ascribed to the formation of excited state aggregates  
13 (excimers or super-exciplexes) under strong laser pumping conditions of high optical density  
14 active media,<sup>45</sup> hence it is absent in the photophysical measurements. In this sense, the laser  
15 band recorded for these dyes at high concentrations in ethyl acetate corresponds to an  
16 aggregated form of the dyes, whereas the blue-shifted laser band at low concentrations  
17 corresponds to the dye in monomeric form (Figure 11). The presence of this kind of  
18 aggregates also enables widening the tuning range.<sup>45b</sup>

19  
20  
21  
22  
23  
24  
25  
26  
27  
28  
29  
30  
31  
32  
33  
34  
35  
36  
37  
38  
39  
40  
41  
42  
43  
44  
45  
46  
47  
48  
49  
50  
51  
52  
53  
54  
55  
56  
57  
58  
59  
60

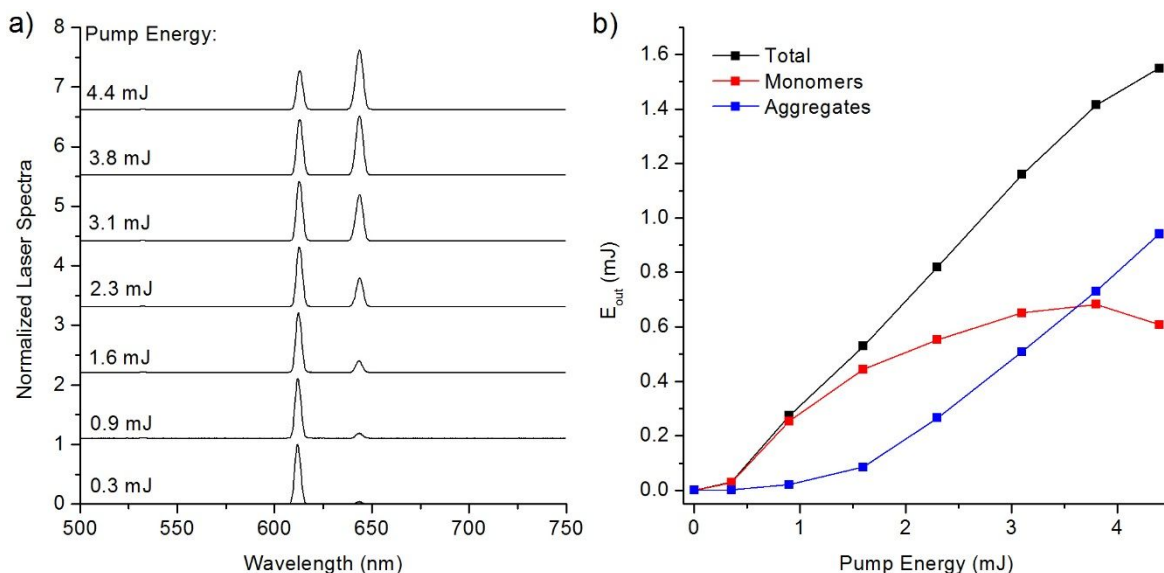


**Figure 11.** Normalized laser spectra (left) and output energy (right) as a function of pump energy for dye **25** 0.38 mM in ethyl acetate.

With regard to the laser efficiencies, those dyes which showed high fluorescence efficiency regardless of the surrounding media (**22**, **23**, **25**, **26**, **34**, **36** and **41**) display high laser efficiencies (surpassing the 40% at the optimal concentration). On the other hand, those dyes which rendered the lowest fluorescence efficiencies (**24** and **37**) show accordingly the worst laser efficiency (lower than 30%). The only exception to such good correlation is dye **35**, which underwent an ICT process. Indeed, in spite of its low fluorescence response, the recorded laser efficiency for **35** places this compound amongst the best ones in this study. Such apparent mismatch can be rationalized considering the shorter excited-state lifetime of such dye, which favors the stimulated radiative deactivation and compensates for the low spontaneous emission probability. An analogous behavior was reported previously for LDS722, a hemicyanine dye with a quantum yield as low as 14% but a 43% laser efficiency owing to a lifetime of around 500 ps.<sup>46</sup> Most of the dyes show a good tolerance to a prolonged and intense laser pumping, with the exception of the dyes bearing methoxy (**25** and **41**) or formyl (**24**) functional groups at *para* position of the 8-phenyl ring. Indeed, more than 3

1  
2  
3 GJ/mol are required to decrease the laser output energy to a 90% of its initial value,  
4  
5 outstanding the fluorinated dye **34**, which is able to tolerate up to 7.4 GJ/mol before the same  
6  
7 energy loss is recorded (Table 6). These results are consistent with a previously reported  
8  
9 strategy based on the fluorination of organic dyes, which enabled achieving long lasting  
10  
11 active media even under drastic pumping regime.<sup>47</sup>  
12  
13

14  
15 To put these results into perspective, we compared the laser performance of these red emitting  
16  
17 laser dyes with that of the commercially available BODIPY PM650, consisting of a  
18  
19 methylated dipyrin core with a cyano group at the *meso* position, that emits in the same  
20  
21 spectral region.<sup>43</sup> This dye is very photostable (tolerance up to 6.3 GJ/mol) owing to the  
22  
23 electron withdrawing character of the said cyano group, which reduces the reactivity against  
24  
25 the oxidizing ambient oxygen, involved in the photodegradation mechanism.<sup>48</sup> At the same  
26  
27 time, such functionalization enables the population of ICT states. Such non-radiative  
28  
29 deactivation channel shortens the lifetime, supporting the recorded moderately high laser  
30  
31 efficiencies (30%, Table 6) in spite of its reduced fluorescence efficiency. The photostability  
32  
33 of most of the herein tested dyes are lower than that of PM650, albeit some of them to reach  
34  
35 close values, outstanding dye **34** whose photostability even surpasses that of the reference  
36  
37 PM650. On the other hand, the recorded laser efficiencies of most of the herein tested dyes  
38  
39 (mainly, **22**, **23**, **25**, **26**, **34**, **36** and **41**) improve that displayed by PM650. Therefore, the  
40  
41 herein reported benzofuran-fused BODIPYs are suitable candidates to develop efficient red-  
42  
43 emitting lasers with a reasonable photostability.  
44  
45  
46  
47  
48  
49  
50

## 51 **Conclusions**

52  
53 We have described a novel synthetic methodology to prepare benzofuran-fused BODIPY  
54  
55 dyes in four steps starting from commercially available 8-methylthioBODIPY **4**. Careful  
56  
57  
58  
59  
60

1  
2  
3 selection of the reaction conditions permitted the chemoselective functionalization of the  
4 *meso*-position of multiply functionalized BODIPY **6**. S<sub>N</sub>Ar-like reaction of phenolates  
5 exclusively at the 3- and 5-positions allow the positioning of such moiety for the final  
6 intramolecular Pd(0)-catalyzed arylation at the 2- and 6-positions of the BODIPY nucleus.  
7  
8 The herein reported synthetic avenue allows not only an easy access to benzofuran-fused  
9 BODIPYs with different substitution pattern, but also enables to incorporate relevant  
10 biomolecules to the BODIPYs core. Once these biomolecules are endowed with new  
11 fluorescent properties, they may find very interesting biology-related applications such as  
12 sensors, cell-imaging, protein-labeling, and so on. The extended aromatic framework of these  
13 conformationally restricted BODIPYs renders strong absorption, fluorescence and laser  
14 bands shifted to the red edge of the visible. Indeed, the fluorescence and laser efficiencies  
15 reach almost the 100% and are above 40%, respectively, in the best cases. It is worthy to note  
16 that the laser emission is rather intriguing displaying a deep shift towards the red edge owing  
17 to the promotion of excited state aggregates at high concentration and under intense laser  
18 pumping. Therefore, these  $\pi$ -extended BODIPYs show nice behavior as red laser dyes in  
19 terms of efficiency and photostability, since up to 7.3 GJ per mol of dye are required to induce  
20 a decrease of the output laser emission of just a 10%, overcoming the limitations of most of  
21 the commercially available dyes (such as cyanines or oxazines) in such spectral region. This  
22 method is amenable to grafting other heterocycles such as indoles and benzothiophenes by  
23 adding either anilines or thiophenols. We are currently exploring these possibilities as well  
24 as the cell-imaging properties of both **41** and **42**. The results will be reported in due course.  
25  
26  
27  
28  
29  
30  
31  
32  
33  
34  
35  
36  
37  
38  
39  
40  
41  
42  
43  
44  
45  
46  
47  
48  
49  
50

## 51 52 53 54 **Experimental** 55 56 57 58 59 60

1  
2  
3 **Photophysical properties:** Spectroscopic properties were registered in diluted solutions  
4 (around  $2 \times 10^{-6}$  M), prepared by adding the corresponding solvent (spectroscopic grade) to  
5 the residue from the adequate amount of a concentrated stock solution in acetone, after  
6 vacuum evaporation of this solvent. UV-Vis absorption, and fluorescence spectra and decay  
7 curves were recorded on a Varian model CARY 4E spectrophotometer and an Edinburgh  
8 Instruments spectrofluorimeter (model FLSP 920), respectively. Fluorescence quantum  
9 yields ( $\phi$ ) were obtained using as reference commercial cresyl violet ( $\phi^r = 0.54$  in methanol).  
10 The values were corrected by the refractive index of the solvent. Radiative decay curves were  
11 registered with the time correlated single-photon counting technique using a multichannel  
12 plate detector with picosecond time-resolution. Fluorescence emission was monitored at the  
13 maximum emission wavelength after excitation by means of a wavelength-tunable Fianium  
14 Supercontinuum laser. The fluorescence lifetime ( $\tau$ ) was obtained after the deconvolution of  
15 the instrumental response signal from the recorded decay curves by means of an iterative  
16 method. The goodness of the exponential fit was controlled by statistical parameters (chi-  
17 square and the analysis of the residuals). The radiative ( $k_{fl}$ ) and non-radiative ( $k_{nr}$ ) rate  
18 constants were calculated from the fluorescence quantum yield and lifetime;  $k_{fl} = \phi/\tau$  and  $k_{nr}$   
19  $= (1-\phi)/\tau$ .

20  
21  
22  
23  
24  
25  
26  
27  
28  
29  
30  
31  
32  
33  
34  
35  
36  
37  
38  
39  
40  
41  
42 **Quantum mechanical calculations:** Ground state geometries were optimized at the Density  
43 Functional Theory (DFT) using range-separated hybrid wB97XD method, whereas the first  
44 singlet excite state was optimized by the Time Dependent (TD) method and the same  
45 functional. In both cases the triple valence basis set with two polarization functions (6-  
46 311g\*\*) was used. The geometries were considered as energy minimum when the  
47 corresponding frequency analysis did not give any negative value. The solvent effect (ethyl  
48  
49  
50  
51  
52  
53  
54  
55  
56  
57  
58  
59  
60

1  
2  
3 acetate) was considered in the conducted theoretical simulations by means of the Polarizable  
4 Continuum Model (PCM). All the calculations were performed using the Gaussian 16  
5 software as implemented in the computational cluster “arina” of the UPV/EHU.  
6  
7

8  
9  
10 **Electrochemistry:** Cyclic voltammograms (Metrohm Autolab) were done using a three-  
11 electrode set up with a platinum layer (surface 8 mm x 7.5 mm) working electrode, platinum  
12 wire as counter electrode and Ag/AgCl as reference electrode. A 0.1 M solution of  
13 tetrabutylammonium hexafluorophosphate (TBAPF<sub>6</sub>) in dry acetonitrile was used as the  
14 electrolyte solvent in which the compounds were dissolved to achieve a concentration of  
15 around 1 mM. All redox potentials were reported vs ferrocene as internal standard. The  
16 solutions were purged with argon and all the measurements were performed under an inert  
17 atmosphere.  
18  
19  
20  
21  
22  
23  
24  
25  
26  
27

28  
29 **Laser measurements set-up:** Liquid solutions of dyes in ethyl acetate were contained in 1  
30 cm optical-path rectangular quartz cells carefully sealed to avoid solvent evaporation during  
31 experiments. The liquid solutions were transversely pumped with 20 ns full width at half  
32 maximum (FWHM) pulses from a frequency-doubled (532nm) Q-switched Nd:YAG laser  
33 (Lotis TII SL-2132) at a repetition rate of 1 Hz. The exciting pulses were line-focused onto  
34 the cell using a combination of positive and negative cylindrical lenses ( $f=15\text{cm}$  and  $f=-$   
35  $15\text{cm}$ , respectively) perpendicularly arranged. The plane parallel oscillation cavity (2 cm  
36 length) consisted of a 90% reflectivity aluminum mirror acting as back reflector, and with  
37 the lateral face of the cell acting as output coupler (4% reflectivity). The pump and output  
38 energies were detected by a calibrated Laser Energy Meter (QE 12LP-S-MB-DO, Gentec).  
39  
40  
41  
42  
43  
44  
45  
46  
47  
48  
49  
50  
51  
52  
53  
54  
55  
56  
57  
58  
59  
60  
The output laser emission was directed towards a fiber bundle and detected with a  
spectrograph/monochromator (Spectrapro-300i Acton Research) equipped with a  
thermoelectrically cooled CCD detector (SpectruMM:GS 128B). A shortwave Cut-off filter

(OptoSigma, cut-off at 540 nm) was placed before the fibre bundle to avoid any scattered pump light entering the spectrograph. Neutral density filters were used to avoid CCD detector saturation.

The photostability of the dyes in ethyl acetate solution was evaluated by using a pumping energy and geometry exactly equal to that of the laser experiments. We used spectroscopic quartz cuvettes with 1 cm optical paths and depths  $L = 0.1$  cm to allow for the minimum solution volume ( $V_S = 60$   $\mu\text{L}$ ) to be excited. The lateral facets were grounded, whereupon no laser oscillation was obtained. Nevertheless, information about photostabilities can be obtained by monitoring the decrease in laser-induced fluorescence (LIF) intensity. In order to facilitate comparisons independently of the experimental conditions and sample, the photostability figure of merit was defined as the accumulated pump energy absorbed by the system ( $E_{\text{dose}}$ ), per mole of dye, before the output energy falls to a 90% its initial value. In terms of experimental parameters, this energy dose, in units of  $\text{GJ mol}^{-1}$ , can be expressed as:

$$E_{\text{dose}}^{90\%} (\text{GJ} \cdot \text{mol}^{-1}) = \frac{E_{\text{pump}} (\text{GJ}) \cdot (1 - 10^{-\varepsilon CL}) \sum_{\text{\#pulses}} f}{CV_S} \quad (1)$$

where  $E_{\text{pump}}$  is the energy per pulse in GJules,  $C$  is the molar concentration,  $\varepsilon$  is the molar absorption coefficient in units of  $\text{M}^{-1} \text{cm}^{-1}$ ,  $L$  is the depth of the cuvette expressed in cm,  $V_S$  is the solution volume, in liters, within the cuvette, and  $f$  is the ratio between the LIF intensity after  $\text{\#pulses}$  and the LIF intensity in the first pulse. It can be shown that  $\sum f$  accounts for the reduction in pump absorption due to species photo-degradation. To speed up the experiment the pump repetition rate was increased up to 15Hz. The fluorescence emission was monitored perpendicular to the exciting beam, collected by an optical fiber, and acquired using the previously described spectrograph/monochromator system.

1  
2  
3 **X-ray Crystal Structure determination:** Intensity data were collected on an Agilent  
4 Technologies Super-Nova diffractometer, which was equipped with monochromated Cu  $\alpha$   
5 radiation ( $\lambda = 1.54184 \text{ \AA}$ ) and Atlas CCD detector. Measurement was carried out at 99.99(10)  
6 K with the help of an Oxford Cryostream 700 PLUS temperature device. Data frames were  
7 processed (unit cell determination, analytical absorption correction with face indexing,  
8 intensity data integration and correction for Lorentz and polarization effects) using the  
9 CrysAlis software package. The structure was solved using Olex2 and refined by full-matrix  
10 least-squares with SHELXL-97. Final geometrical calculations were carried out with  
11 Mercury and PLATON as integrated in WinGX. Crystallographic data (excluding structure  
12 factors) for the structure(s) reported in this paper have been deposited with the Cambridge  
13 Crystallographic Data Centre as supplementary publication no. CCDC-1877155. Copies of  
14 the data can be obtained free of charge from [www.ccdc.cam.ac.uk/conts/retrieving.html](http://www.ccdc.cam.ac.uk/conts/retrieving.html).  
15  
16  
17  
18  
19  
20  
21  
22  
23  
24  
25  
26  
27  
28  
29  
30  
31  
32  
33  
34

35 **Synthesis and characterization:**  $^1\text{H}$  and  $^{13}\text{C}$  NMR spectra were recorded in  
36 deuteriochloroform ( $\text{CDCl}_3$ ), with either tetramethylsilane (TMS) (0.00 ppm  $^1\text{H}$ , 0.00 ppm  
37  $^{13}\text{C}$ ), chloroform (7.26 ppm  $^1\text{H}$ , 77.00 ppm  $^{13}\text{C}$ ). Data are reported in the following order:  
38 chemical shift in ppm, multiplicities (br (broadened), s (singlet), d (doublet), t (triplet), q  
39 (quartet), m (multiplet), exch (exchangeable), app (apparent)), coupling constants,  $J$  (Hz),  
40 and integration. Infrared spectra were recorded on a FTIR spectrophotometer. Peaks are  
41 reported ( $\text{cm}^{-1}$ ) with the following relative intensities: s (strong, 67–100 %), m (medium, 40–  
42 67%), and w (weak, 20–40%). Melting points are not corrected. TLC was conducted in Silica  
43 gel on TLC Al foils. Detection was done by UV light (254 or 365 nm). HRMS samples were  
44 ionized by ESI+ and recorded via the TOF method.  
45  
46  
47  
48  
49  
50  
51  
52  
53  
54  
55  
56  
57  
58  
59  
60

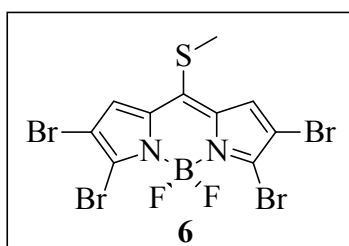
1  
2  
3 **Materials.** Starting 8-methylthioBODIPY, CuTC, tri(2-furyl)phosphine, and boronic acids  
4 are commercially available. Solvents were dried and distilled before use.  
5  
6

7  
8 **General Procedure for the L–S Cross-Coupling reaction (GP1).** A Schlenk tube  
9 equipped with a stir bar was charged with **6** (1.0 equiv), the corresponding boronic acid (3.0  
10 equiv), and dry THF (0.03 M). The mixture was sparged with N<sub>2</sub> for 3 min, whereupon  
11 Pd<sub>2</sub>(dba)<sub>3</sub> (2.5 mol %), trifurylphosphine (7.5%), and CuTC (3.0 equiv) were added under  
12 N<sub>2</sub>. The Schlenk tube was then immersed in a preheated oil bath at 55 °C. The oil bath was  
13 removed after the starting material **6** BODIPY was consumed (TLC, AcOEt/hexanes). After  
14 the mixture reached rt, the solvent was removed and the crude material was adsorbed in SiO<sub>2</sub>  
15 gel, dried under reduced pressure, and purified by flash chromatography on SiO<sub>2</sub> gel using  
16 AcOEt/hexanes as eluent.  
17  
18  
19  
20  
21  
22  
23  
24  
25  
26  
27

28 **General Procedure for the nucleophilic substitution with phenols and phenol**  
29 **derivatives (GP2).** A sealed tube with a stir bar was charged with the corresponding  
30 BODIPYs (**10-15**) (1.0 equiv), phenol or phenol derivatives (4 or 6 equiv), Na<sub>2</sub>CO<sub>3</sub> (5 or 6  
31 equiv) and acetonitrile (0.02M), then the mixture was sparged with N<sub>2</sub> during 5 minutes. The  
32 tube was sealed, and the solution was stirred at 110 °C until completion (TLC monitoring,  
33 AcOEt/hexanes, THF/hexane or acetone/hexane as indicate). The oil bath was removed after  
34 the starting BODIPY was consumed. After the mixture reached rt, the solvent was removed  
35 under reduced pressure, and the crude material was adsorbed in SiO<sub>2</sub> gel, dried under vacuum  
36 and purified by flash chromatography on SiO<sub>2</sub> gel using THF/hexanes, acetone/hexanes,  
37 CHCl<sub>3</sub>/hexanes or AcOEt/hexanes as indicated.  
38  
39  
40  
41  
42  
43  
44  
45  
46  
47  
48  
49  
50

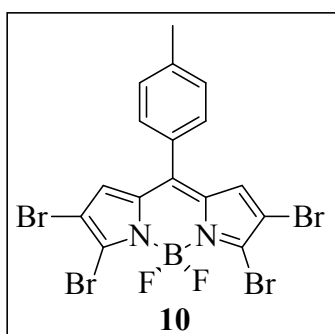
51 **General Procedure for the cyclization reaction (GP3).** A sealed tube with a stir bar  
52 was charged with the corresponding BODIPY (**16-21, 27-33**) (1.0 equiv), Pd(OAc)<sub>2</sub> (0.05  
53 equiv), PPh<sub>3</sub> (0.1 equiv), K<sub>2</sub>CO<sub>3</sub> (3 equiv) and toluene, then the mixture was sparged with N<sub>2</sub>  
54  
55  
56  
57  
58  
59  
60

during 5 min. The tube was sealed, and the solution was stirred at 150 °C until completion (TLC monitoring, AcOEt/hexanes, THF/hexane or CHCl<sub>3</sub>/hexane as indicate). The oil bath was removed after the starting BODIPY was consumed. After the mixture reached rt, the solvent was removed under reduced pressure, and the crude material was adsorbed in SiO<sub>2</sub> gel, dried under vacuum and purified by flash chromatography on SiO<sub>2</sub> gel using acetone/hexanes or CHCl<sub>3</sub>/hexanes as indicated.



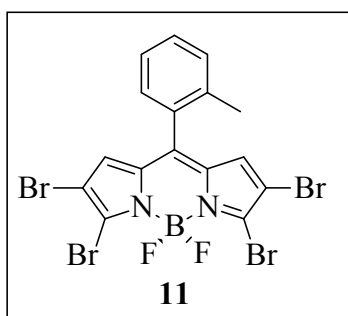
**Synthesis of 6.** A round-bottom flask under N<sub>2</sub> was charged with **4** (30 mg, 0.126 mmol, 1 equiv), *N*-bromosuccinimide (112.1 mg, 0.63 mmol, 5.0 equiv) and acetic acid (4.2 mL). The reaction mixture was stirred at room temperature

overnight whereupon water (30 mL) was added and the pH was adjusted using saturated Na<sub>2</sub>CO<sub>3</sub> to pH 7. The product was extracted with ethyl acetate, washed with brine (5 x 20 mL), dried with anhyd. MgSO<sub>4</sub>, and filtered. The solvent was removed under reduced pressure, and the crude product was adsorbed in SiO<sub>2</sub> gel, dried under vacuum, and purified by flash chromatography using 10% EtOAc/hexanes. The desired product (20 mg, 0.036 mmol, 70%) was obtained as a dark red solid. TLC (15% EtOAc/hexanes, R<sub>f</sub> = 0.25); mp 212-214°C; IR (KBr, cm<sup>-1</sup>): 2669 (w), 1516 (s), 1441 (m), 1364 (s), 1335 (s), 1303 (m), 1237 (s), 1161 (s), 1097 (s), 979 (m), 966 (m), 916 (s), 819 (w), 808 (w), 744 (w), 632 (w), 587 (w), 502 (w); <sup>1</sup>H NMR (500 MHz, CDCl<sub>3</sub>) δ 7.44 (s, 2H), 2.83 (s, 3H). <sup>13</sup>C {<sup>1</sup>H} (126 MHz, CDCl<sub>3</sub>): δ 147.7, 134.9, 133.5, 128.7, 111.8, 21.5. HRMS (ESI+) *m/z* calcd for C<sub>10</sub>H<sub>5</sub>BBr<sub>4</sub>F<sub>2</sub>N<sub>2</sub>SK [M+K]<sup>+</sup> 592.6560. Found 592.6547.



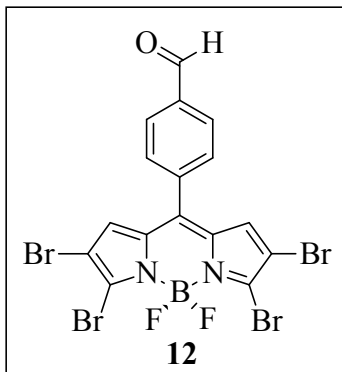
**Synthesis of 10.**<sup>49</sup> According to GP1. **6** (25 mg, 0.045 mmol), *p*-tolylboronic acid (18.4 mg, 0.135 mmol), Pd<sub>2</sub>(dba)<sub>3</sub> (1.0 mg, 1.1 × 10<sup>-3</sup> mmol), TFP (0.79 mg, 3.4 × 10<sup>-3</sup> mmol), and CuTC

(25.8 mg, 0.135 mmol). After 2 h the crude was purified using 0.2% AcOEt/hexanes. The desired product (13 mg, 0.022 mmol, 48%) was obtained as dark red solid. TLC (20% THF/hexanes,  $R_f = 0.79$ ); mp  $>260^\circ\text{C}$  decompose.;  $^1\text{H}$  NMR (500 MHz,  $\text{CDCl}_3$ ):  $\delta$  7.38 (d,  $J = 8.1$  Hz, 2H), 7.35 (d,  $J = 8.2$  Hz, 2H), 6.93 (s, 2H), 2.47 (s, 3H). HRMS (ESI+)  $m/z$  calcd for  $\text{C}_{17}\text{H}_{10}\text{BBr}_4\text{F}_2\text{N}_2$   $[\text{M}+\text{H}]^+$  598.7596. Found 598.7619.



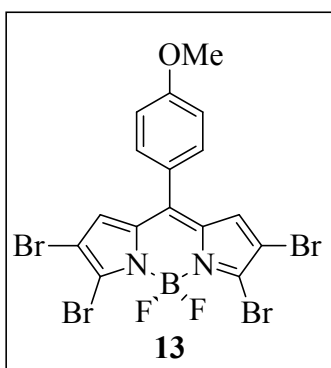
**Synthesis of 11.** According to GP1. **6** (20 mg, 0.036 mmol), *o*-tolylboronic acid (14.7 mg, 0.108 mmol),  $\text{Pd}_2(\text{dba})_3$  (0.82 mg,  $9.0 \times 10^{-4}$  mmol), TFP (0.63 mg,  $2.7 \times 10^{-3}$  mmol), and CuTC (20.7 mg, 0.108 mmol). After 2 h the crude material was purified using 3% AcOEt/hexanes. The desired product (16.5

mg, 0.027 mmol, 76% yield) was obtained as dark red crystals. TLC (20% AcOEt/hexanes,  $R_f = 0.57$ ); mp  $>260^\circ\text{C}$  dec.; IR (KBr,  $\text{cm}^{-1}$ ): 3679 (w), 2921 (w), 2661 (w), 1554 (s), 1539 (s), 1488 (m), 1452 (w), 1354 (s), 1312 (s), 1247 (s), 1225 (s), 1179 (s), 1141 (s), 1083 (s), 1014 (m), 999 (m), 905 (m), 839 (m), 819 (m), 737 (s), 701 (m), 651 (w), 597 (w), 543 (w), 488 (w);  $^1\text{H}$  NMR (500 MHz,  $\text{CDCl}_3$ ):  $\delta$  7.45 (t,  $J = 7.1$  Hz, 2H), 7.35 - 7.28 (m, 2H), 7.21 (d,  $J = 7.4$  Hz, 2H), 6.68 (s, 2H), 2.23 (s, 3H).  $^{13}\text{C}$  { $^1\text{H}$ } (126 MHz,  $\text{CDCl}_3$ )  $\delta$  142.5, 136.6, 135.7, 135.4, 131.0, 131.0, 130.9, 130.6, 129.9, 125.9, 112.3, 20.2. HRMS (ESI+)  $m/z$  calcd for  $\text{C}_{16}\text{H}_{10}\text{BBr}_4\text{F}_2\text{N}_2$   $[\text{M}+\text{H}]^+$  598.7596. Found 598.7620.



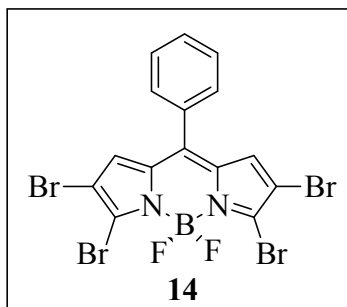
**Synthesis of 12.** According to GP1. **6** (10 mg, 0.02 mmol), *p*-formylphenyl boronic acid (5.4 mg, 0.04 mmol), Pd<sub>2</sub>(dba)<sub>3</sub> (0.4 mg, 5.0 × 10<sup>-4</sup> mmol), TFP (0.3 mg, 1.4 × 10<sup>-3</sup> mmol), and CuTC (10.3 mg, 0.05 mmol). After 1 h the crude material was purified using 5% AcOEt/hexanes. The desired product (4.2 mg, 0.007 mmol, 38% yield) was obtained as green crystals.

TLC (15% AcOEt/hexanes, R<sub>f</sub> = 0.46); mp 271-272 °C; IR (KBr, cm<sup>-1</sup>): 3679 (w), 3120 (w), 1701 (s), 1573 (s), 1551 (s), 1447 (w), 1357 (s), 1314 (m), 1287 (w), 1238 (s), 1207 (w), 1179 (w), 1097 (s), 1018 (w), 995 (m), 833 (m), 753 (m), 705 (m), 652 (w), 486 (w); <sup>1</sup>H NMR (500 MHz, CDCl<sub>3</sub>): δ 10.15 (s, 1H), 8.07 (d, *J* = 8.0 Hz, 2H), 7.67 (d, *J* = 8.0 Hz, 2H), 6.85 (s, 3H). <sup>13</sup>C{<sup>1</sup>H} (126 MHz, CDCl<sub>3</sub>): δ 191.0, 140.5, 138.2, 137.3, 136.6, 134.7, 131.3, 131.0, 130.0, 112.8. HRMS (ESI<sup>+</sup>) *m/z* calcd for C<sub>16</sub>H<sub>7</sub>BBr<sub>4</sub>F<sub>2</sub>N<sub>2</sub>ONa [M+Na]<sup>+</sup> 634.7208. Found 634.7212.



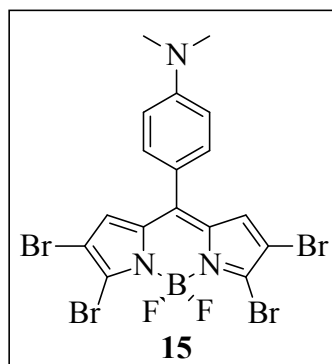
**Synthesis of 13.**<sup>50</sup> According to GP1. **6** (20 mg, 0.036 mmol), *p*-methoxyphenyl boronic acid (16.5 mg, 0.108 mmol), Pd<sub>2</sub>(dba)<sub>3</sub> (0.83 mg, 9.0 × 10<sup>-4</sup> mmol), TFP (0.63 mg, 2.7 × 10<sup>-3</sup> mmol), and CuTC (20.7 mg, 0.11 mmol). After 3 h the crude was purified using 15% AcOEt/hexanes. The desired product (14 mg, 0.023 mmol, 63% yield) was obtained as dark red solid.

TLC (20% AcOEt/hexanes, R<sub>f</sub> = 0.5); mp 238-239 °C; <sup>1</sup>H NMR (500 MHz, CDCl<sub>3</sub>): δ 7.46 (d, *J* = 8.7 Hz, 2H), 7.06 (d, *J* = 8.7 Hz, 2H), 6.95 (s, 2H), 3.92 (s, 3H). HRMS (ESI<sup>+</sup>) *m/z* calcd for C<sub>16</sub>H<sub>9</sub>BBr<sub>4</sub>F<sub>2</sub>N<sub>2</sub>ONa [M+Na]<sup>+</sup> 636.7366. Found 636.7364.



**Synthesis of 14.**<sup>50</sup> According to GP1. **6** (50 mg, 0.090 mmol), phenylboronic acid (40.0 mg, 0.072 mmol), Pd<sub>2</sub>(dba)<sub>3</sub> (1.7 mg,  $1.8 \times 10^{-3}$  mmol), TFP (1.3 mg,  $5.4 \times 10^{-3}$  mmol), and CuTC (41.3 mg, 0.260 mmol). After 2 h the crude was purified using 1% AcOEt/hexane. The desired product (9.5 mg, 0.016 mmol,

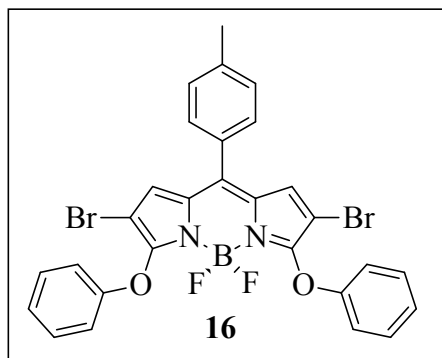
18%) was obtained as purple solid. TLC (10% AcOEt/hexanes,  $R_f = 0.48$ ); mp >200 °C dec.; <sup>1</sup>H NMR (500 MHz, CDCl<sub>3</sub>): δ 7.63 (t,  $J = 7.4$  Hz, 1H), 7.55 (t,  $J = 7.6$  Hz, 2H), 7.48 (d,  $J = 7.2$  Hz, 2H), 6.90 (s, 1H). HRMS (ESI+)  $m/z$  calcd for C<sub>15</sub>H<sub>7</sub>BBr<sub>4</sub>F<sub>2</sub>N<sub>2</sub>Na [M+Na]<sup>+</sup> 606.7259. Found 606.7278.



**Synthesis of 15.** According to GP1. **6** (50 mg, 0.09 mmol), 4-(dimethylamino)phenyl boronic acid (44.7 mg, 0.27 mmol), Pd<sub>2</sub>(dba)<sub>3</sub> (2.07 mg,  $2.3 \times 10^{-3}$  mmol), TFP (1.6 mg,  $6.8 \times 10^{-3}$  mmol), and CuTC (51.7 mg, 0.27 mmol). After 50 min the crude material was purified using 30% AcOEt/hexanes. The desired product (30 mg, 0.048 mmol, 53% yield) was obtained as dark

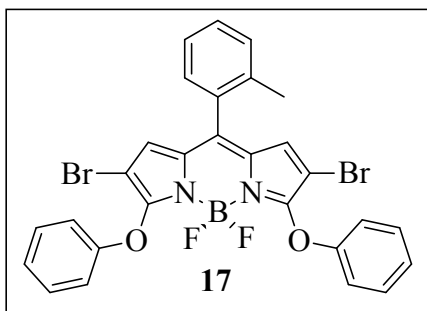
blue solid. TLC (20% AcOEt/hexanes,  $R_f = 0.2$ ); mp 221-223 °C; IR (KBr, cm<sup>-1</sup>): 2918 (w), 1602 (s), 1542 (w), 1512 (m), 1493 (m), 1431 (w), 1403 (w), 1361 (s), 1328 (m), 1283 (m), 1254 (m), 1195 (m), 1106 (m), 1004 (w), 984 (m), 976 (m), 826 (w), 751 (w), 647 (w), 537 (w); <sup>1</sup>H NMR (500 MHz, CDCl<sub>3</sub>): δ 7.45 (d,  $J = 8.8$  Hz, 2H), 7.01 (s, 2H), 6.79 (d,  $J = 8.8$  Hz, 2H), 3.13 (s, 3H). <sup>13</sup>C{<sup>1</sup>H} (126 MHz, CDCl<sub>3</sub>): δ 153.3, 144.4, 134.3, 133.4, 131.6,

1  
2  
3 131.0, 119.9, 112.0, 110.8, 40.3. HRMS (ESI+)  $m/z$  calcd for  $C_{17}H_{13}BBr_4F_2N_3$   $[M+H]^+$   
4  
5 627.7862. Found 627.7854.  
6  
7  
8  
9



**Synthesis of 16.** According to GP2. **10** (46.0 mg, 0.08 mmol), phenol (36.2 mg, 0.39 mmol),  $Na_2CO_3$  (40.8 mg, 0.39 mmol) and acetonitrile (4 mL). The reaction mixture was stirred at 110 °C for 6 h. The crude was purified using 1% AcOEt/hexanes. The desired

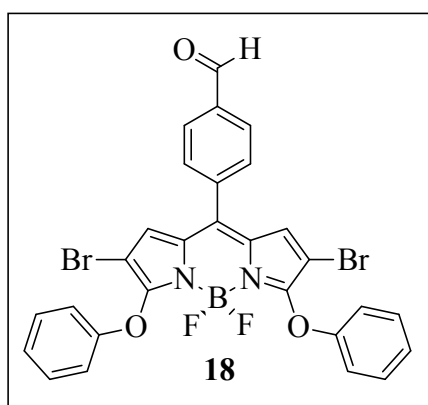
product (19.4 mg, 0.032 mmol, 80% yield) was obtained as red crystals. TLC (10% AcOEt/hexanes,  $R_f$  = 0.26); mp 197-199 °C; IR (KBr,  $cm^{-1}$ ): 3679 (w), 2971 (w), 1571 (m), 1553 (m), 1546 (m), 1501 (m), 1485 (m), 1448 (s), 1333 (w), 1253 (s), 1204 (w), 1181 (m), 1128 (s), 1038 (s), 1003 (w), 988 (w), 840 (m), 711 (w);  $^1H$  NMR (500 MHz,  $CDCl_3$ ):  $\delta$  7.44 (d,  $J$  = 8.0 Hz, 2H), 7.38 - 7.30 (m, 6H), 7.16 - 7.09 (m, 6H), 6.94 (s, 2H), 2.48 (s, 2H).  $^{13}C$  { $^1H$ } (126 MHz,  $CDCl_3$ ):  $\delta$  157.9, 155.8, 142.6, 141.6, 132.1, 130.5, 129.8, 129.6, 129.5, 127.7, 124.6, 117.9, 96.1, 21.6. HRMS (ESI+)  $m/z$  calcd for  $C_{28}H_{19}BBr_2F_2N_2O_2Na$   $[M+Na]^+$   
37 646.9753. Found 646.9743.  
38  
39  
40  
41



**Synthesis of 17.** According to GP2. **11** (43.0 mg, 0.07 mmol), phenol (33.8 mg, 0.36 mmol),  $Na_2CO_3$  (38.1 mg, 0.36 mmol) and acetonitrile (4 mL). The reaction mixture was stirred at 110 °C for 3 h. The crude was purified using 1% AcOEt/hexanes. The desired product

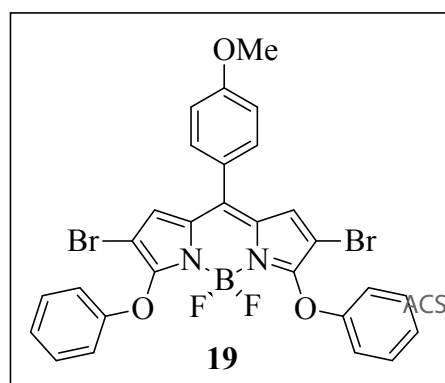
(34.6 mg, 0.055 mmol, 77% yield) was obtained as red crystals. TLC (10% AcOEt/hexanes,  $R_f$  = 0.30); mp 202-203 °C; IR (KBr,  $cm^{-1}$ ): 3672 (w), 2972 (w), 2917 (w), 1563 (m), 1485

(m), 1450 (s), 1352 (w), 1337 (w), 1251 (s), 1197 (m), 1182 (m), 1118 (s), 1034 (s), 1003 (w), 912 (w), 839 (m), 741 (m), 706 (w), 685 (w);  $^1\text{H}$  NMR (500 MHz,  $\text{CDCl}_3$ ):  $\delta$  7.46 - 7.41 (m, 1H), 7.37 - 7.27 (m, 7H), 7.17 - 7.10 (m, 6H), 6.69 (s, 2H), 2.31 (s, 3H).  $^{13}\text{C}\{^1\text{H}\}$  (126 MHz,  $\text{CDCl}_3$ ):  $\delta$  158.1, 155.7, 141.7, 136.9, 131.5, 131.4, 130.8, 130.3, 130.1, 129.8, 128.1, 125.7, 124.7, 118.0, 96.2, 20.2. HRMS (ESI+)  $m/z$  calcd for  $\text{C}_{28}\text{H}_{20}\text{BBr}_2\text{F}_2\text{N}_2\text{O}_2$   $[\text{M}]^+$  624.9933. Found 624.9934.



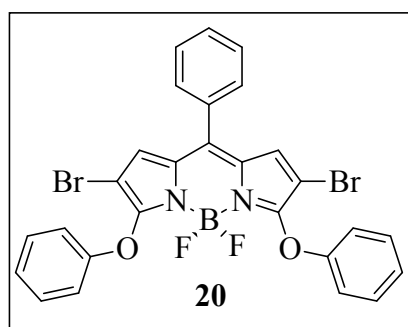
**Synthesis of 18.** According to GP2. **12** (20.0 mg, 0.03 mmol), phenol (18.5 mg, 0.20 mmol),  $\text{Na}_2\text{CO}_3$  (20.8 mg, 0.20 mmol) and acetonitrile (2 mL). The reaction mixture was stirred at 110 °C for 3 h. The crude material was purified using 10% AcOEt/hexanes. The desired product (12.0 mg, 0.019 mmol, 57% yield) was

obtained as red crystals. TLC (20% AcOEt/hexanes,  $R_f$  = 0.30); mp 112-113 °C; IR (KBr,  $\text{cm}^{-1}$ ): 3694 (w), 2973 (w), 1704 (m), 1574 (m), 1556 (m), 1500 (m), 1450 (s), 1350 (w), 1253 (s), 1201 (m), 1182 (m), 1123 (s), 1037 (s), 1003 (m), 833 (m), 757 (w), 686 (w);  $^1\text{H}$  NMR (500 MHz,  $\text{CDCl}_3$ ):  $\delta$  10.15 (s, 1H), 8.07 (d,  $J$  = 8.2 Hz, 2H), 7.72 (d,  $J$  = 8.1 Hz, 2H) 7.37 - 7.30 (m, 4H), 7.16 (t,  $J$  = 7.4 Hz, 2H), 7.13 - 7.10 (m, 4H), 6.86 (s, 2H).  $^{13}\text{C}\{^1\text{H}\}$  (126 MHz,  $\text{CDCl}_3$ ):  $\delta$  191.3, 158.6, 155.6, 139.8, 138.0, 137.8, 131.8, 131.1, 129.9, 129.9, 127.4, 124.9, 118.0, 96.7. HRMS (ESI+)  $m/z$  calcd for  $\text{C}_{28}\text{H}_{18}\text{BBr}_2\text{F}_2\text{N}_2\text{O}_3$   $[\text{M}+\text{H}]^+$  638.9726. Found 638.9730.



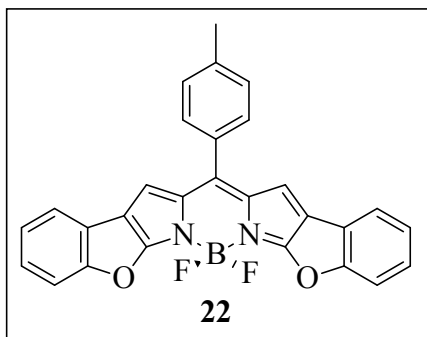
**Synthesis of 19.** According to GP2. **13** (34.5 mg, 0.06 mmol), phenol (26.4 mg, 0.29 mmol),  $\text{Na}_2\text{CO}_3$  (29.8

1  
2  
3 mg, 0.28 mmol) and acetonitrile (3 mL). The reaction mixture was stirred at 110 °C for 5.5  
4  
5 h. The crude material was purified using 2% AcOEt/hexanes. The desired product (25.9 mg,  
6  
7 0.040 mmol, 72% yield) was obtained as orange crystals. TLC (10% AcOEt/hexanes,  $R_f$  =  
8  
9 0.08); mp 237-238 °C; IR (KBr,  $\text{cm}^{-1}$ ): 3694 (w), 2972 (w), 2917 (w), 2845 (w), 1605 (w),  
10  
11 1575 (m), 1551 (s), 1500 (m), 1485 (m), 1452 (s), 1444 (s), 1351 (w), 1333 (w), 1297 (w),  
12  
13 1256 (s), 1182 (s), 1130 (s), 1108 (s), 1039 (s), 1020 (m), 838 (s), 716 (m), 684 (w), 606 (w),  
14  
15 575 (w);  $^1\text{H}$  NMR (500 MHz,  $\text{CDCl}_3$ ):  $\delta$  7.50 (d,  $J$  = 8.7 Hz, 2H), 7.35 - 7.30 (m, 4H), 7.17  
16  
17 - 7.05 (m, 8H), 6.96 (s, 2H), 3.92 (s, 3H).  $^{13}\text{C}$  { $^1\text{H}$ } (126 MHz,  $\text{CDCl}_3$ ):  $\delta$  162.2, 157.7, 155.9,  
18  
19 142.4, 132.3, 132.0, 129.8, 127.6, 124.7, 124.6, 117.9, 114.5, 96.0, 55.73. HRMS (ESI+)  $m/z$   
20  
21 calcd for  $\text{C}_{28}\text{H}_{20}\text{BBr}_2\text{F}_2\text{N}_2\text{O}_3$   $[\text{M}+\text{H}]^+$  640.9883. Found 640.9867.



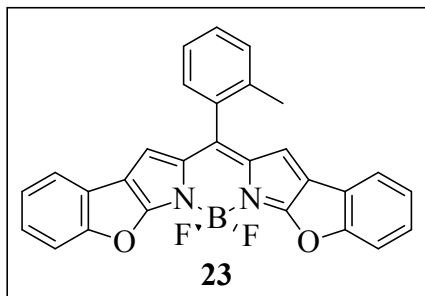
**Synthesis of 20.** According to GP2. **14** (31 mg, 0.05  
mmol), phenol (25 mg, 0.27 mmol),  $\text{Na}_2\text{CO}_3$  (28.1  
mg, 0.27 mmol) and acetonitrile (2.5 mL). The reaction  
mixture was stirred at 110 °C for 3 h. The crude material  
was purified using 2% AcOEt/hexanes. The desired

product (38.4 mg, 0.062 mmol, 60% yield) was obtained as red crystals. TLC (10%  
AcOEt/hexanes,  $R_f$  = 0.30); mp 213-214 °C; IR (KBr,  $\text{cm}^{-1}$ ): 3368 (w), 2972 (w), 1578 (w),  
1551 (s), 1502 (m), 1485 (m), 1451 (s), 1440 (s), 1333 (w), 1289 (w), 1253 (s), 1206 (w),  
1182 (m), 1123 (s), 1038 (s), 1003 (w), 988 (w), 840 (m), 731 (w), 718 (w), 605 (w);  $^1\text{H}$   
NMR (500 MHz,  $\text{CDCl}_3$ ):  $\delta$  7.62 - 7.58 (m, 1H), 7.35 - 7.31 (m, 4H), 7.16 - 7.09 (m, 6H),  
6.92 (s, 2H).  $^{13}\text{C}$  { $^1\text{H}$ } (126 MHz,  $\text{CDCl}_3$ ):  $\delta$  158.1, 155.8, 142.2, 132.3, 132.1, 130.9, 130.5,  
129.8, 128.9, 127.7, 124.7, 117.9, 96.2. HRMS (ESI+)  $m/z$  calcd for  $\text{C}_{27}\text{H}_{18}\text{BBr}_2\text{F}_2\text{N}_2\text{O}_2$   
 $[\text{M}+\text{H}]^+$  610.9777. Found 610.9767.



**Synthesis of 22.** According to GP3. **16** (30.0 mg, 0.05 mmol), Pd(OAc)<sub>2</sub> (0.54 mg, 2.4 × 10<sup>-3</sup> mmol, 0.05 equiv), PPh<sub>3</sub> (1.3 mg, 4.8 × 10<sup>-3</sup> mmol, 0.1 equiv), K<sub>2</sub>CO<sub>3</sub> (19.9 mg, 0.14 mmol, 3 equiv) and toluene (4 mL). The reaction mixture was stirred at 150 °C for 7

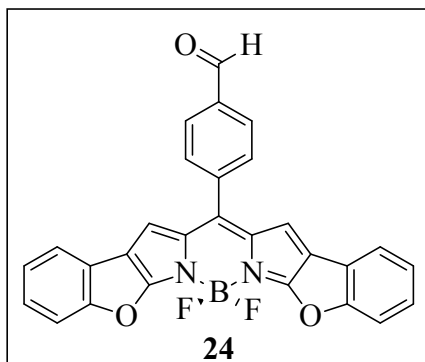
h. The crude material was purified using 80% CHCl<sub>3</sub>/hexanes. The desired product (13.0 mg, 0.04 mmol, 59% yield) was obtained as a golden solid. TLC (20% THF/hexanes, R<sub>f</sub> = 0.3); mp 263-265 °C; IR (KBr, cm<sup>-1</sup>): 2921 (w), 1628 (w), 1577 (s), 1478 (m), 1449 (s), 1442 (s), 1408 (s), 1367 (s), 1348 (s), 1323 (s), 1291 (m), 1277 (m), 1186 (w), 1159 (m), 1143 (s), 1113 (s), 1012 (w), 987 (s), 926 (w), 818 (m), 808 (m), 760 (w), 743 (m), 714 (w), 696 (w), 555 (m), 467 (w); <sup>1</sup>H NMR (500 MHz, CDCl<sub>3</sub>): δ 7.60 - 7.50 (m, 6H), 7.38 (d, *J* = 7.7 Hz, 2H), 7.33 (t, *J* = 7.3 Hz, 2H), 7.29 - 7.24 (m, 3H), 6.87 (s, 2H), 2.51 (s, 3H). <sup>13</sup>C{<sup>1</sup>H} (126 MHz, CDCl<sub>3</sub>): δ 167.4, 161.0, 145.9, 140.8, 134.6, 130.9, 130.5, 129.3, 126.6, 124.7, 121.6, 121.6, 118.7, 118.1, 113.2, 21.6. HRMS (ESI+) *m/z* calcd for C<sub>28</sub>H<sub>18</sub>BF<sub>2</sub>N<sub>2</sub>O<sub>2</sub> [M+H]<sup>+</sup> 463.1429. Found 463.1419.



**Synthesis of 23.** According to GP3. **17** (30.0 mg, 0.05 mmol), Pd(OAc)<sub>2</sub> (0.54 mg, 2.4 × 10<sup>-3</sup> mmol, 0.05 equiv), PPh<sub>3</sub> (1.3 mg, 4.8 × 10<sup>-3</sup> mmol, 0.1 equiv), K<sub>2</sub>CO<sub>3</sub> (19.9, 0.14 mmol, 3 equiv) and toluene (4 mL). The reaction mixture was stirred at 150 °C for 6 h. The crude

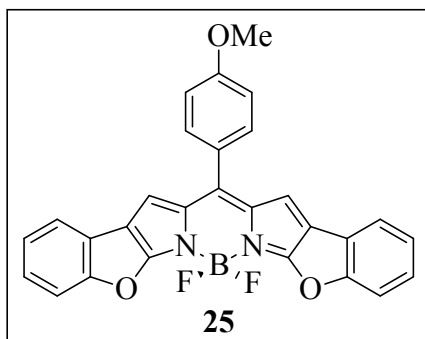
was purified using 60% CHCl<sub>3</sub>/hexanes. The desired product (14.7 mg, 0.04 mmol, 66% yield) was obtained as a golden solid. TLC (60% CHCl<sub>3</sub>/hexanes, R<sub>f</sub> = 0.3); mp >300 °C

dec.; IR (KBr,  $\text{cm}^{-1}$ ): 3352 (w), 3066 (w), 2972 (w), 1627 (m), 1578 (s), 1477 (m), 1448 (s), 1441 (s), 1344 (s), 1319 (s), 1292 (s), 1185 (w), 1158 (s), 1140 (s), 1107 (s), 1012 (m), 985 (s), 818 (s), 762 (m), 745 (m), 737 (m), 702 (m), 554 (m), 529 (m), 476 (w);  $^1\text{H}$  NMR (500 MHz,  $\text{CDCl}_3$ ):  $\delta$  7.56 - 7.52 (m, 4H), 7.47 (t,  $J = 8.2$  Hz, 1H), 7.41 - 7.30 (m, 5H), 7.28 - 7.23 (m, 3H), 6.63 (s, 2H), 2.33 (s, 3H).  $^{13}\text{C}\{^1\text{H}\}$  (126 MHz,  $\text{CDCl}_3$ ):  $\delta$  167.6, 161.1, 144.9, 137.3, 134.8, 132.5, 130.6, 130.6, 129.8, 126.7, 125.6, 124.7, 121.7, 121.5, 118.4, 118.0, 113.2, 20.1. HRMS (ESI+)  $m/z$  calcd for  $\text{C}_{28}\text{H}_{18}\text{BF}_2\text{N}_2\text{O}_2$   $[\text{M}+\text{H}]^+$  463.1429. Found 463.1438.



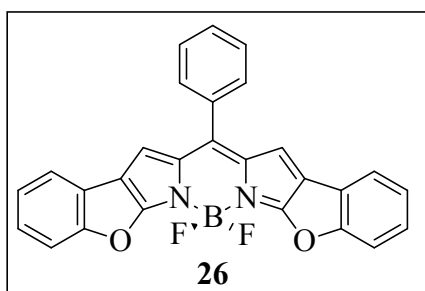
**Synthesis of 24.** According to GP3. **18** (25.0 mg, 0.04 mmol),  $\text{Pd}(\text{OAc})_2$  (0.44 mg,  $1.9 \times 10^{-3}$  mmol, 0.05 equiv),  $\text{PPh}_3$  (1.0 mg,  $3.9 \times 10^{-3}$  mmol, 0.1 equiv),  $\text{K}_2\text{CO}_3$  (16.2 mg, 0.12 mmol, 3 equiv) and toluene (4 mL). The reaction mixture was stirred at 150  $^\circ\text{C}$  for 5 h. The crude product was purified using 30%  $\text{CHCl}_3$ /hexanes. The desired

product (12.5 mg, 0.03 mmol, 67% yield) was obtained as a golden solid. TLC (30%  $\text{CHCl}_3$ /hexanes,  $R_f = 0.1$ ); mp  $>300$   $^\circ\text{C}$  dec.; IR (KBr,  $\text{cm}^{-1}$ ): 3116 (w), 3063 (w), 2971 (w), 2732 (w), 1705 (s), 1627 (s), 1557 (s), 1479 (s), 1450 (s), 1442 (s), 1415 (m), 1377 (s), 1355 (s), 1324 (m), 1292 (w), 1191 (w), 1161 (m), 1144 (s), 1118 (s), 1110 (s), 1013 (s), 992 (s), 820 (s), 810 (w), 751 (m), 697 (m), 557 (m);  $^1\text{H}$  NMR (500 MHz,  $\text{CDCl}_3$ ):  $\delta$  10.19 (s, 1H), 8.10 (d,  $J = 8.1$  Hz, 2H), 7.83 (d,  $J = 8.0$  Hz, 2H), 7.56 (t,  $J = 8.9$  Hz, 4H), 7.35 (t,  $J = 8.5$  Hz, 2H), 7.30 - 7.26 (m, 2H), 6.77 (s, 2H).  $^{13}\text{C}\{^1\text{H}\}$  (126 MHz,  $\text{CDCl}_3$ ):  $\delta$  191.5, 167.9, 161.2, 143.3, 139.2, 137.6, 134.2, 131.5, 129.8, 127.1, 124.9, 121.8, 121.3, 118.9, 118.2, 113.3. HRMS (ESI+)  $m/z$  calcd for  $\text{C}_{28}\text{H}_{15}\text{BF}_2\text{N}_2\text{O}_3$   $[\text{M}]^+$  476.1143. Found 476.1154.



**Synthesis of 25.** According to GP3. **19** (20.0 mg, 0.03 mmol), Pd(OAc)<sub>2</sub> (0.35 mg, 1.6 x 10<sup>-3</sup> mmol, 0.05 equiv), PPh<sub>3</sub> (0.82 mg, 3.1 x 10<sup>-3</sup> mmol, 0.1 equiv), K<sub>2</sub>CO<sub>3</sub> (12.9 mg, 0.094 mmol, 3 equiv) and toluene (4 mL). The reaction mixture was stirred at 150 °C for 6 h.

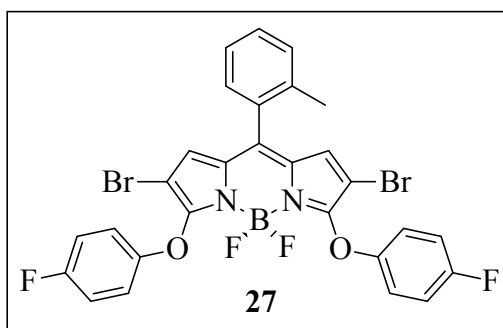
The crude material was purified using 80% CHCl<sub>3</sub>/hexanes. The desired product (7.2 mg, 0.02 mmol, 48% yield) was obtained as a golden solid. TLC (20% THF/hexanes, R<sub>f</sub> = 0.4); mp 297-299 °C; IR (KBr, cm<sup>-1</sup>): 2970 (w), 2926 (w), 2854 (w), 1735 (w), 1627 (w), 1605 (w), 1577 (s), 1478 (m), 1449 (s), 1442 (s), 1371 (s), 1356 (s), 1292 (m), 1252 (m), 1180 (w), 1159 (s), 1144 (s), 1114 (s), 1012 (m), 989 (s), 818 (m), 761 (w), 746 (w), 697 (w), 556 (w); <sup>1</sup>H NMR (500 MHz, CDCl<sub>3</sub>): δ 7.61 - 7.53 (m, 6H), 7.33 (t, *J* = 8.5 Hz, 2H), 7.29 - 7.26 (m, 2H), 7.10 (d, *J* = 8.6 Hz, 2H), 6.89 (s, 2H), 3.94 (s, 3H). <sup>13</sup>C{<sup>1</sup>H} (126 MHz, CDCl<sub>3</sub>): δ 167.2, 161.7, 161.0, 145.7, 134.5, 132.4, 126.6, 125.8, 124.7, 121.7, 121.6, 118.6, 118.1, 114.2, 113.2, 55.7. HRMS (ESI+) *m/z* calcd for C<sub>28</sub>H<sub>17</sub>BF<sub>2</sub>N<sub>2</sub>O<sub>3</sub> [M]<sup>+</sup> 478.1300, found 478.1322.



**Synthesis of 26.** According to GP3. **20** (30.0 mg, 0.05 mmol), Pd(OAc)<sub>2</sub> (0.55 mg, 2.4 x 10<sup>-3</sup> mmol, 0.05 equiv), PPh<sub>3</sub> (1.3 mg, 4.9 x 10<sup>-3</sup> mmol, 0.1 equiv), K<sub>2</sub>CO<sub>3</sub> (20.4 mg, 0.15 mmol, 3 equiv) and toluene (4 mL). The reaction mixture was stirred at 150 °C for 6 h. The crude

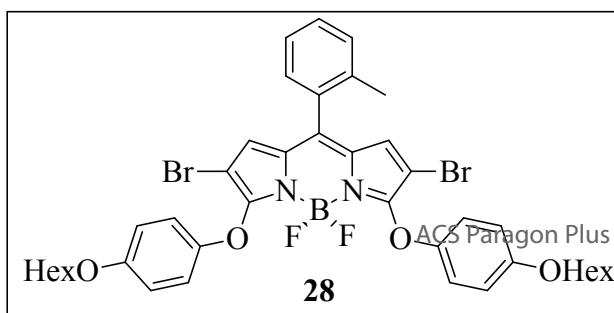
material was purified using 60% CHCl<sub>3</sub>/hexanes. The desired product (15.9 mg, 0.03 mmol, 72% yield) was obtained as a golden solid. TLC (20% THF/hexanes, R<sub>f</sub> = 0.4); mp >290 °C dec.; IR (KBr, cm<sup>-1</sup>): 2972 (w), 1628 (w), 1578 (s), 1478 (m), 1448 (s), 1345 (s), 1324 (s),

1  
2  
3 1292 (m), 1185 (w), 1159 (s), 1143 (s), 1108 (s), 1012 (w), 983 (s), 926 (w), 819 (s), 762  
4 (w), 747 (w), 721 (m), 554 (m), 519 (w);  $^1\text{H NMR}$  (500 MHz,  $\text{CDCl}_3$ ):  $\delta$  7.66 - 7.54 (m, 9H),  
5 7.34 (t,  $J = 8.5$  Hz, 2H), 7.29 - 7.24 (m, 2H), 6.85 (s, 2H).  $^{13}\text{C}\{^1\text{H}\}$  (126 MHz,  $\text{CDCl}_3$ ):  $\delta$   
6 167.5, 161.1, 145.6, 134.6, 133.4, 130.8, 130.4, 128.6, 126.7, 124.7, 121.7, 121.6, 118.7,  
7 118.3, 113.2. HRMS (ESI+)  $m/z$  calcd for  $\text{C}_{27}\text{H}_{16}\text{BF}_2\text{N}_2\text{O}_2$   $[\text{M}+\text{H}]^+$  449.1272. Found  
8 449.1271.  
9  
10  
11  
12  
13  
14  
15  
16  
17  
18



**Synthesis of 27.** According to GP2. **11** (30.0 mg, 0.05 mmol), *p*-fluorophenol (33.8 mg, 0.30 mmol),  $\text{Na}_2\text{CO}_3$  (31.9 mg, 0.30 mmol) and acetonitrile (2.5 mL). The reaction mixture was stirred at 110 °C for 2 h. The crude material was

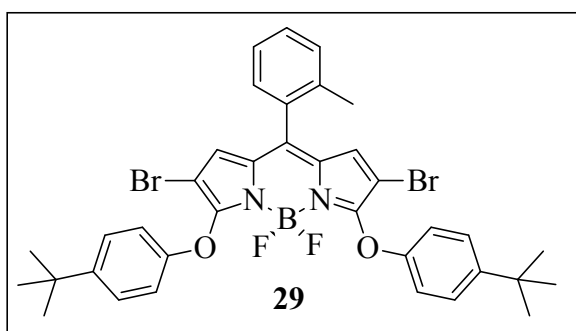
30 purified using 15% AcOEt/hexanes. The desired product (26.1 mg, 0.039 mmol, 79% yield)  
31 was obtained as red crystals. TLC (20% THF/hexanes,  $R_f = 0.55$ ); mp 89-91 °C; IR (KBr,  
32  $\text{cm}^{-1}$ ): 3121 (w), 2922 (w), 1564 (s), 1504 (s), 1491 (s), 1449 (s), 1351 (w), 1337 (w), 1252  
33 (s), 1190 (s), 1175 (s), 1119 (s), 1033 (s), 1010 (s), 994 (s), 911 (m), 860 (m), 835 (m), 791  
34 (m), 741 (m), 704 (m), 573 (w), 514 (w);  $^1\text{H NMR}$  (500 MHz,  $\text{CDCl}_3$ ):  $\delta$  7.46 - 7.42 (m, 1H),  
35 7.36 - 7.27 (m, 3H), 7.13 - 7.07 (m, 4H), 7.05 - 7.00 (m, 4H), 6.69 (s, 2H), 2.29 (s, 3H).  $^{13}\text{C}$   
36  $\{^1\text{H}\}$  (126 MHz,  $\text{CDCl}_3$ ):  $\delta$  160.7, 158.7, 158.1, 151.6, 151.5, 136.8, 131.8, 131.2, 130.8,  
37 130.3, 130.2, 125.8, 119.6, 119.5, 116.5, 116.3, 95.9, 20.2. HRMS (ESI+)  $m/z$  calcd for  
38  $\text{C}_{28}\text{H}_{18}\text{BBr}_2\text{F}_4\text{N}_2\text{O}_2$   $[\text{M}+\text{H}]^+$  660.9745. Found 660.9772.  
39  
40  
41  
42  
43  
44  
45  
46  
47  
48  
49  
50  
51  
52



**Synthesis of 28.** According to GP2. **11** (30.0 mg, 0.05 mmol), 4-

HexO- ACS Paragon Plus Environment

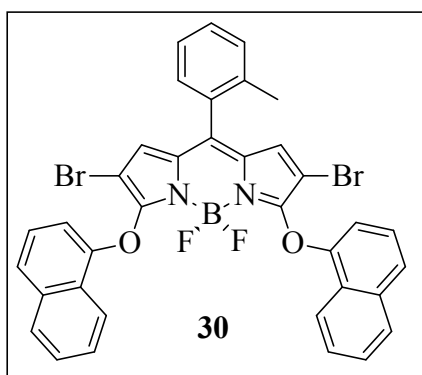
(hexyloxy)phenol (58.5 mg, 0.30 mmol), Na<sub>2</sub>CO<sub>3</sub> (31.9 mg, 0.30 mmol) and acetonitrile (2.5 mL). The reaction mixture was stirred at 110 °C for 2 h. The crude material was purified using 60% CHCl<sub>3</sub>/hexanes. The desired product (37.2 mg, 0.045 mmol, 90% yield) was obtained as red oil. TLC (15% DCM/hexanes, R<sub>f</sub> = 0.90); IR (KBr, cm<sup>-1</sup>): 3694 (w), 2952 (s), 2929 (s), 2870 (s), 2858 (s), 1565 (s), 1493 (s), 1450 (s), 1350 (w), 1337 (w), 1295 (w), 1251 (s), 1213 (s), 1193 (s), 1178 (s), 1118 (s), 1033 (s), 1007 (m), 994 (m), 831 (m), 793 (w), 740 (m), 706 (m), 610 (w), 515 (w); <sup>1</sup>H NMR (500 MHz, CDCl<sub>3</sub>): δ 7.42 (t, *J* = 8.8 Hz, 1H), 7.35 - 7.25 (m, 3H), 7.06 (d, *J* = 9.1 Hz, 4H), 6.83 (d, *J* = 9.1 Hz, 4H), 6.63 (s, 2H), 3.91 (t, *J* = 6.6 Hz, 4H), 2.28 (s, 3H), 1.79 - 1.71 (m, 4H), 1.50 - 1.40 (m, 4H), 1.37 - 1.27 (m, 8H), 0.90 (t, *J* = 6.9 Hz, 6h). <sup>13</sup>C{<sup>1</sup>H} (126 MHz, CDCl<sub>3</sub>): δ 158.4, 156.3, 149.3, 140.9, 136.9, 131.5, 131.5, 130.7, 130.3, 130.0, 127.8, 125.7, 119.3, 115.3, 95.5, 68.6, 31.7, 29.4, 25.8, 22.7, 20.2, 14.2. HRMS (ESI+) *m/z* calcd for C<sub>40</sub>H<sub>44</sub>BBr<sub>2</sub>F<sub>2</sub>N<sub>2</sub>O<sub>4</sub> [M+H]<sup>+</sup> 825.1714. Found 825.1730.



**Synthesis of 29.** According to GP2. **11** (30.0 mg, 0.05 mmol), 4-*tert*-butylphenol (45.2 mg, 0.30 mmol), Na<sub>2</sub>CO<sub>3</sub> (31.9 mg, 0.30 mmol) and acetonitrile (2.5 mL). The reaction mixture was stirred at 110 °C for 1

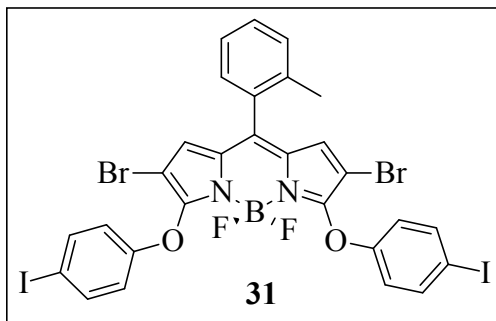
h. The crude was purified using 15% THF/hexanes. The desired product (33.3 mg, 0.045 mmol, 90% yield) was obtained as red solid. TLC (20% THF/hexanes, R<sub>f</sub> = 0.68); mp 108-110 °C; IR (KBr, cm<sup>-1</sup>): 3681 (w), 2962 (m), 2864 (w), 1564 (m), 1494 (m), 1451 (s), 1364 (w), 1351 (w), 1334 (w), 1252 (s), 1215 (m), 1194 (m), 1120 (s), 1033 (s), 1013 (w), 830 (w), 741 (w), 699 (w), 549 (w); <sup>1</sup>H NMR (500 MHz, CDCl<sub>3</sub>): δ 7.43 (t, *J* = 8.1 Hz, 1H), 7.36

1  
2  
3 - 7.27 (m, 7H), 7.02 (d,  $J = 8.8$  Hz, 4H), 6.67 (s, 2H), 2.30 (s, 3H), 1.29 (s, 18H).  $^{13}\text{C}\{^1\text{H}\}$   
4  
5 (126 MHz,  $\text{CDCl}_3$ ):  $\delta$  158.2, 153.5, 147.5, 141.3, 136.9, 131.4, 131.3, 130.7, 130.3, 130.1,  
6  
7 128.0, 126.6, 125.7, 117.2, 96.3, 34.5, 31.6, 20.2. HRMS (ESI+)  $m/z$  calcd for  
8  $\text{C}_{36}\text{H}_{36}\text{BBr}_2\text{F}_2\text{N}_2\text{O}_2$   $[\text{M}+\text{H}]^+$  737.1188. Found 737.1203.  
9



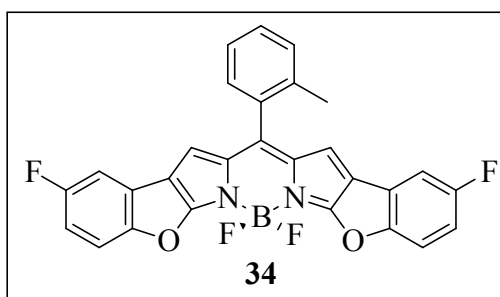
**Synthesis of 30.** According to GP2. **11** (30.0 mg, 0.05 mmol), 1-naphthol (28.9 mg, 0.20 mmol),  $\text{Na}_2\text{CO}_3$  (21.3 mg, 0.20 mmol) and acetonitrile (2.5 mL). The reaction mixture was stirred at 110 °C for 1 h. The crude material was purified using 20% THF/hexanes. The desired product (29.3 mg, 0.040 mmol, 81% yield) was obtained

32 as purple solid. TLC (20% THF/hexanes,  $R_f = 0.3$ ); mp 223-225 °C; IR (KBr,  $\text{cm}^{-1}$ ): 3673  
33 (w), 3113 (w), 3055 (w), 1599 (w), 1560 (s), 1492 (s), 1455 (s), 1389 (s), 1349 (w), 1248 (s),  
34  
35 1223 (s), 1178 (m), 1132 (s), 1072 (s), 1044 (s), 1013 (s), 878 (m), 791 (w), 771 (m), 742  
36  
37 (m), 703 (m), 541 (w);  $^1\text{H}$  NMR (500 MHz,  $\text{CDCl}_3$ ):  $\delta$  8.33 - 8.31 (m, 2H), 7.86 - 7.82 (m,  
38 2H), 7.65 (d,  $J = 8.3$  Hz, 2H), 7.57 - 7.49 (m, 4H), 7.48 - 7.42 (m, 1H), 7.40 - 7.31 (m, 5H),  
39 7.04 (d,  $J = 7.6$  Hz, 2H), 6.72 (s, 2H), 2.36 (s, 3H).  $^{13}\text{C}\{^1\text{H}\}$  (126 MHz,  $\text{CDCl}_3$ ):  $\delta$  158.4,  
40 151.4, 141.3, 136.8, 134.6, 131.4, 131.3, 130.7, 130.2, 130.0, 128.0, 127.5, 126.9, 126.4,  
41 125.6, 125.5, 125.2, 124.7, 121.9, 112.2, 95.7, 20.1. HRMS (ESI+)  $m/z$  calcd for  
42  $\text{C}_{36}\text{H}_{24}\text{BBr}_2\text{F}_2\text{N}_2\text{O}_2$   $[\text{M}+\text{H}]^+$  725.0249. Found 725.0267.  
43  
44  
45  
46  
47  
48  
49  
50  
51  
52  
53  
54  
55  
56  
57  
58  
59  
60



**Synthesis of 31.** According to GP2. **11** (30.0 mg, 0.05 mmol), 4-iodophenol (66.3 mg, 0.30 mmol, 6 equiv), Na<sub>2</sub>CO<sub>3</sub> (31.9 mg, 0.30 mmol, 6 equiv) and acetonitrile (2.5 mL). The reaction mixture was stirred at 110 °C for 2 h. The crude material

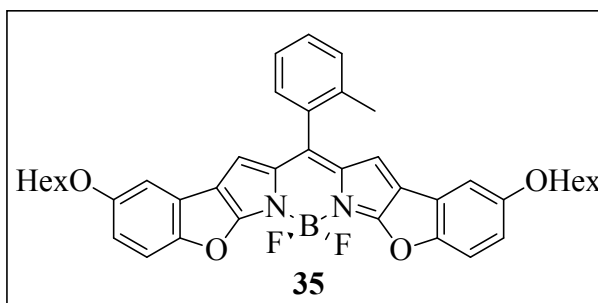
was purified using 10% THF/hexanes. The desired product (25.6 mg, 0.03 mmol, 58% yield) was obtained as red solid. TLC (20% THF/hexanes,  $R_f = 0.6$ ); mp 106-107 °C; IR (KBr, cm<sup>-1</sup>): 3680 (w), 2972 (w), 1561 (s), 1496 (m), 1477 (s), 1448 (s), 1351 (w), 1336 (w), 1252 (s), 1216 (s), 1202 (s), 1186 (m), 1120 (s), 1033 (s), 1006 (s), 911 (w), 839 (w), 823 (w), 741 (w), 707 (w), 687 (w), 541 (w), 488 (w); <sup>1</sup>H NMR (500 MHz, CDCl<sub>3</sub>): δ 7.63 (d,  $J = 8.9$  Hz, 4H), 7.44 (t,  $J = 8.2$  Hz, 1H), 7.37 - 7.26 (m, 3H), 6.87 (d,  $J = 8.9$  Hz, 4H), 6.70 (s, 2H), 2.29 (s, 3H). <sup>13</sup>C {<sup>1</sup>H} (126 MHz, CDCl<sub>3</sub>): δ 157.6, 155.6, 142.5, 138.8, 136.8, 131.7, 131.1, 130.9, 130.3, 130.3, 128.2, 125.8, 120.0, 96.4, 88.1, 20.3. HRMS (ESI+)  $m/z$  calcd for C<sub>28</sub>H<sub>18</sub>BBr<sub>2</sub>F<sub>2</sub>I<sub>2</sub>N<sub>2</sub>O<sub>2</sub> [M+H]<sup>+</sup> 876.7866. Found 876.7868.



**Synthesis of 34.** According to GP3. **27** (23.0 mg, 0.04 mmol), Pd(OAc)<sub>2</sub> (0.39 mg, 1.7 x 10<sup>-3</sup> mmol, 0.05 equiv), PPh<sub>3</sub> (0.91 mg, 3.5 x 10<sup>-3</sup> mmol, 0.1 equiv), K<sub>2</sub>CO<sub>3</sub> (14.4 mg, 0.104 mmol, 3 equiv) and toluene (4 mL). The reaction mixture was stirred

at 150 °C for 6 h. The crude material was purified using 60% CHCl<sub>3</sub>/hexanes. The desired product (13.3 mg, 0.03 mmol, 75%) was obtained as a golden solid. TLC (20% THF/hexanes,  $R_f = 0.6$ ); mp >300 °C; IR (KBr, cm<sup>-1</sup>): 3401 (w), 2972 (w), 1635 (m), 1579 (s), 1474 (w), 1459 (m), 1374 (s), 1312 (s), 1265 (w), 1168 (w), 1137 (s), 1101 (s), 1072 (w), 993 (s), 966

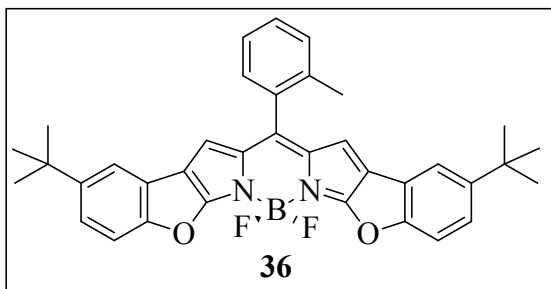
(m), 860 (w), 804 (w), 771 (w), 740 (w), 699 (w), 601 (w), 563 (w), 507 (w);  $^1\text{H}$  NMR (500 MHz,  $\text{CDCl}_3$ ):  $\delta$  7.50 - 7.45 (m, 3H), 7.41 - 7.33 (m, 3H), 7.22 (dd,  $J = 8.0, 2.7$  Hz, 2H), 7.03 (td,  $J = 8.9, 2.7$  Hz, 2H), 6.66 (s, 2H), 2.32 (s, 3H).  $^{13}\text{C}\{^1\text{H}\}$  (126 MHz,  $\text{CDCl}_3$ ):  $\delta$  168.2, 161.0, 159.1, 156.9, 156.9, 145.9, 137.2, 135.0, 132.1, 130.7, 130.5, 130.0, 125.7, 122.5, 122.4, 118.8, 118.1, 113.8, 113.8, 113.7, 113.5, 108.5, 108.3, 20.1. HRMS (ESI+)  $m/z$  calcd for  $\text{C}_{28}\text{H}_{16}\text{BF}_4\text{N}_2\text{O}_2$   $[\text{M}+\text{H}]^+$  499.1240. Found 499.1238.



**Synthesis of 35.** According to GP3. **28**

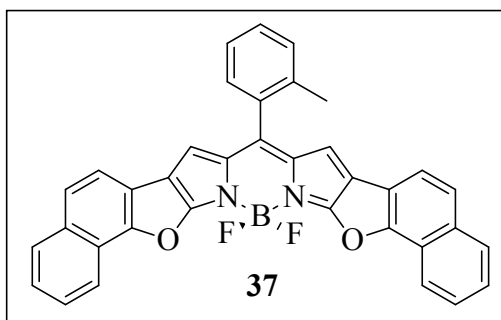
(40.0 mg, 0.05 mmol),  $\text{Pd}(\text{OAc})_2$  (0.54 mg,  $2.4 \times 10^{-3}$  mmol, 0.05 equiv),  $\text{PPh}_3$  (1.3 mg,  $4.8 \times 10^{-3}$  mmol, 0.1 equiv),  $\text{K}_2\text{CO}_3$  (20.1 mg, 0.15 mmol, 3 equiv) and

toluene (4 mL). The reaction mixture was stirred at 150 °C for 7 h. The crude material was purified using 40%  $\text{CHCl}_3$ /hexanes. The desired product (22.3 mg, 0.03 mmol, 69%) was obtained as a golden solid. TLC (20% THF/hexanes,  $R_f = 0.7$ ); mp 205-206 °C; IR (KBr,  $\text{cm}^{-1}$ ): 3066 (w), 2934 (m), 2868 (m), 1635 (m), 1577 (s), 1465 (s), 1460 (s), 1452 (s), 1415 (m), 1350 (s), 1316 (s), 1275 (s), 1207 (s), 1150 (s), 1106 (s), 993 (s), 965 (s), 945 (m), 871 (w), 858 (w), 828 (w), 778 (m), 742 (m), 701 (m), 691 (m), 580 (m), 494 (m);  $^1\text{H}$  NMR (500 MHz,  $\text{CDCl}_3$ ):  $\delta$  7.45 (t,  $J = 8.2$  Hz, 1H), 7.42 - 7.31 (m, 5H), 7.03 (d,  $J = 2.0$  Hz, 2H), 6.85 (dd,  $J = 9.0, 2.6$  Hz, 2H), 6.58 (s, 2H), 3.94 (t,  $J = 6.6$  Hz, 4H), 2.32 (s, 3H), 1.85 - 1.71 (m, 4H), 1.49 - 1.41 (m, 4H), 1.39 - 1.25 (m, 8H), 0.9 (t,  $J = 7.0$  Hz, 6H).  $^{13}\text{C}\{^1\text{H}\}$  (126 MHz,  $\text{CDCl}_3$ ):  $\delta$  168.1, 156.6, 155.5, 144.6, 137.2, 134.7, 132.5, 130.6, 130.5, 129.7, 125.5, 122.0, 118.7, 117.8, 113.7, 113.4, 106.9, 69.0, 31.7, 29.4, 25.8, 22.7, 20.1, 14.2. HRMS (ESI+)  $m/z$  calcd for  $\text{C}_{40}\text{H}_{42}\text{BF}_2\text{N}_2\text{O}_4$   $[\text{M}+\text{H}]^+$  663.3207. Found 663.3194.



**Synthesis of 36.** According to GP3. **29** (26.0 mg, 0.04 mmol), Pd(OAc)<sub>2</sub> (0.4 mg, 1.8 x 10<sup>-3</sup> mmol, 0.05 equiv), PPh<sub>3</sub> (0.9 mg, 3.5 x 10<sup>-3</sup> mmol, 0.1 equiv), K<sub>2</sub>CO<sub>3</sub> (14.6 mg, 0.11 mmol, 3 equiv) and toluene (4 mL). The

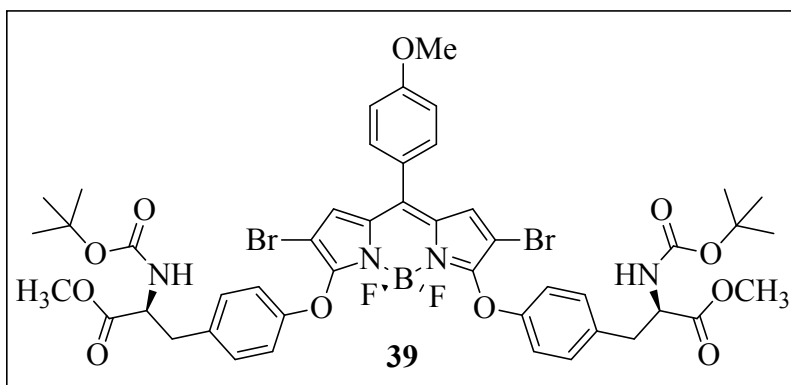
reaction mixture was stirred at 150 °C for 6 h. The crude material was purified using 60% CHCl<sub>3</sub>/hexanes. The desired product (13.0 mg, 0.02 mmol, 64% yield) was obtained as a golden solid. TLC (15% AcOEt/hexanes, R<sub>f</sub> = 0.5); mp 250-252 °C; IR (KBr, cm<sup>-1</sup>): 3684 (w), 2960 (m), 2906 (m), 2868 (m), 1632 (m), 1575 (s), 1460 (s), 1404 (m), 1356 (s), 1342 (s), 1311 (m), 1291 (m), 1168 (s), 1124 (s), 1099 (s), 993 (s), 962 (m), 857 (w), 816 (s), 742 (w), 697 (m), 596 (w), 562 (w), 517 (w), 461 (w); <sup>1</sup>H NMR (500 MHz, CDCl<sub>3</sub>): δ 7.55 (d, *J* = 2.0 Hz, 2H), 7.46 - 7.42 (m, 3H), 7.41 - 7.30 (m, 5H), 6.61 (s, 2H), 2.33 (s, 3H), 1.34 (s, 18H). <sup>13</sup>C{<sup>1</sup>H} (126 MHz, CDCl<sub>3</sub>): δ 167.9, 159.2, 147.9, 144.3, 137.3, 134.7, 132.6, 130.6, 130.5, 129.7, 125.5, 124.1, 121.1, 118.7, 118.5, 117.6, 112.3, 35.0, 31.8, 20.1. HRMS (ESI+) *m/z* calcd for C<sub>36</sub>H<sub>34</sub>BF<sub>2</sub>N<sub>2</sub>O<sub>2</sub> [M+H]<sup>+</sup> 575.2683. Found 575.2675.



**Synthesis of 37.** According to GP3. **30** (30.0 mg, 0.04 mmol), Pd(OAc)<sub>2</sub> (0.5 mg, 2.07 x 10<sup>-3</sup> mmol, 0.05 equiv), PPh<sub>3</sub> (1.1 mg, 4.1 x 10<sup>-3</sup> mmol, 0.1 equiv), K<sub>2</sub>CO<sub>3</sub> (17.2 mg, 0.12 mmol, 3 equiv) and toluene (4 mL). The reaction mixture was stirred

at 150 °C for 7 h. The crude material was purified using 30% CHCl<sub>3</sub>/hexanes. The desired product (8.4 mg, 0.01 mmol, 36% yield) was obtained as golden crystals. TLC (60%

CHCl<sub>3</sub>/hexanes,  $R_f = 0.4$ ); mp >300 °C; IR (KBr, cm<sup>-1</sup>): 3058 (w), 2970 (w), 1639 (w), 1606 (m), 1580 (s), 1558 (m), 1461 (m), 1438 (m), 1390 (s), 1373 (s), 1357 (s), 1335 (s), 1279 (m), 1262 (m), 1144 (s), 1131 (s), 1026 (s), 1005 (s), 965 (s), 847 (m), 803 (m), 736 (m), 696 (m), 671 (w), 602 (w), 582 (w), 560 (w), 503 (w), 457 (w); <sup>1</sup>H NMR (500 MHz, CDCl<sub>3</sub>): δ 8.42 (d,  $J = 8.3$  Hz, 2H), 7.92 (d,  $J = 8.2$  Hz, 2H), 7.72 (d,  $J = 8.4$  Hz, 2H) 7.68 - 7.60 (m, 4H), 7.54 (t,  $J = 8.0$  Hz, 2H), 7.49 (t,  $J = 8.2$  Hz, 1H), 7.45 (d,  $J = 6.6$  Hz, 1H), 7.43 - 7.34 (m, 2H), 6.67 (s, 2H), 2.37 (s, 3H). <sup>13</sup>C{<sup>1</sup>H} (126 MHz, CDCl<sub>3</sub>): δ 167.5, 156.6, 145.3, 137.3, 135.1, 132.8, 132.6, 130.7, 130.6, 129.8, 128.5, 127.3, 126.4, 125.6, 125.1, 121.8, 120.9, 119.5, 119.1, 117.3, 116.9, 20.2. HRMS (ESI+)  $m/z$  calcd for C<sub>36</sub>H<sub>21</sub>BF<sub>2</sub>N<sub>2</sub>O<sub>2</sub>K [M+K]<sup>+</sup> 601.1302. Found 601.1288.

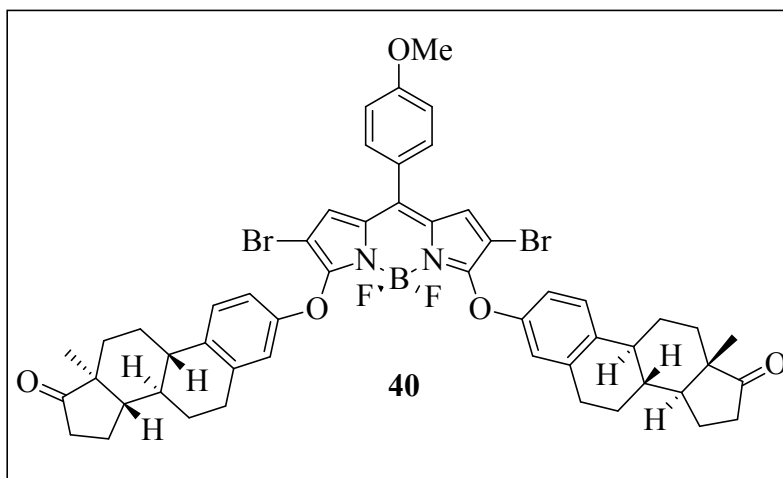


### Synthesis of 39.

According to GP2. **13** (30.0 mg, 0.05 mmol), *N*-(*tert*-butoxycarbonyl)-L-tyrosine methyl ester (86.6 mg, 0.29 mmol, 6 equiv),

Na<sub>2</sub>CO<sub>3</sub> (31.1 mg, 0.29 mmol, 6 equiv) and acetonitrile (2.5 mL). The reaction mixture was stirred at 110 °C for 1 h. The crude material was purified using 20% acetone/hexanes. The desired product (36.0 mg, 0.034 mmol, 71% yield) was obtained as a red solid. TLC (20% acetone/hexanes,  $R_f = 0.9$ ); mp 106-108 °C; IR (KBr, cm<sup>-1</sup>): 3666 (w), 2975 (w), 1743 (m), 1713 (s), 1605 (w), 1575 (m), 1555 (m), 1510 (m), 1492 (s), 1450 (s), 1366 (w), 1350 (w), 1255 (s), 1209 (m), 1179 (m), 1164 (m), 1127 (s), 1037 (m), 1016 (m), 993 (w), 854 (w), 835 (w), 760 (w), 706 (w); <sup>1</sup>H NMR (500 MHz, CDCl<sub>3</sub>): δ 7.49 (d,  $J = 8.7$  Hz, 2H), 7.10 - 7.00

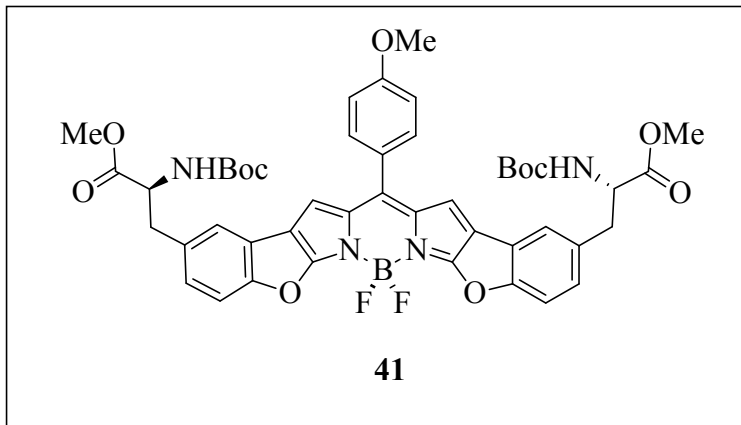
(m, 10H), 6.94 (s, 2H), 4.94 (d,  $J = 8.1$  Hz, 2H), 4.54 (dd,  $J = 13.7, 6.1$  Hz, 2H), 3.91 (s, 3H), 3.65 (s, 6H), 3.10 - 2.99 (m, 4H), 1.41 (s, 18H).  $^{13}\text{C}\{^1\text{H}\}$  (126 MHz,  $\text{CDCl}_3$ ):  $\delta$  172.3, 162.2, 157.6, 155.2, 154.9, 142.4, 132.4, 132.2, 132.0, 130.6, 127.5, 124.6, 118.0, 114.5, 95.8, 80.1, 55.7, 54.6, 52.3, 37.8, 28.4. HRMS (ESI+)  $m/z$  calcd for  $\text{C}_{46}\text{H}_{50}\text{BBr}_2\text{F}_2\text{N}_4\text{O}_{11}$   $[\text{M}+\text{H}]^+$  1043.1891. Found 1043.1884.



**Synthesis of 40.** According to GP2. **13** (30.0 mg, 0.05 mmol), estrone (79.3 mg, 0.29 mmol, 6 equiv),  $\text{Na}_2\text{CO}_3$  (31.1 mg, 0.29 mmol, 6 equiv) and acetonitrile (2.5 mL). The

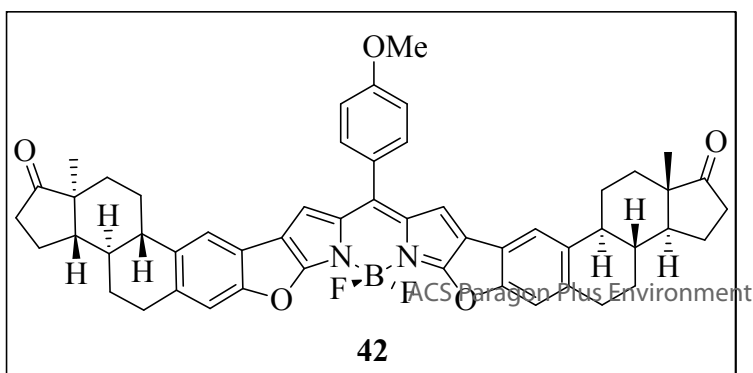
reaction mixture was stirred at 110 °C for 1 h. The crude material was purified using 40% AcOEt/hexanes. The desired product (34.0 mg, 0.034 mmol, 70% yield) was obtained as a red solid. TLC (40% acetone/hexanes,  $R_f = 0.2$ ); mp 180-182 °C; IR (KBr,  $\text{cm}^{-1}$ ): 2929 (s), 2862 (s), 1738 (s), 1605 (s), 1576 (s), 1554 (s), 1487 (s), 1450 (s), 1349 (m), 1297 (w), 1252 (s), 1225 (s), 1202 (s), 1179 (s), 1123 (s), 1036 (s), 993 (m), 928 (m), 913 (s), 837 (w), 819 (w), 792 (w), 763 (w), 732 (w), 707 (w), 634 (w), 548 (w);  $^1\text{H}$  NMR (500 MHz,  $\text{CDCl}_3$ ):  $\delta$  7.50 (d,  $J = 7.8$  Hz, 2H), 7.20 (d,  $J = 8.5$  Hz, 2H), 7.06 (d,  $J = 7.8$  Hz, 2H), 6.95 (s, 2H), 6.85 - 6.79 (m, 4H), 3.92 (s, 3H), 2.86 (d,  $J = 5.2$  Hz, 4H), 2.50 (dd,  $J = 19.1, 8.7$  Hz, 2H), 2.40 - 2.33 (m, 2H), 2.29 - 2.22 (m, 2H), 2.18 - 2.09 (m, 2H), 2.07 - 1.91 (m, 6H), 1.69 - 1.37 (m, 15H), 0.91 (s, 6H).  $^{13}\text{C}\{^1\text{H}\}$  (126 MHz,  $\text{CDCl}_3$ ):  $\delta$  220.9, 162.1, 157.6, 153.9, 142.2, 138.3, 135.8, 132.2, 131.8, 127.6, 126.6, 124.8, 117.4, 114.7, 114.4, 96.2, 55.7, 50.6, 48.1, 44.2,

38.2, 36.0, 31.7, 29.6, 26.5, 25.9, 21.7, 14.0. HRMS (ESI+)  $m/z$  calcd for  $C_{52}H_{52}BBr_2F_2N_2O_5$   
 [M+H]<sup>+</sup> 993.2293. Found 993.2271.



**Synthesis of 41.** According to  
 GP3. **39** (35.0 mg, 0.03 mmol),  
 Pd(OAc)<sub>2</sub> (0.4 mg, 1.68 x 10<sup>-3</sup>  
 mmol, 0.05 equiv), PPh<sub>3</sub> (0.9  
 mg, 3.4 x 10<sup>-3</sup> mmol, 0.1  
 equiv), K<sub>2</sub>CO<sub>3</sub> (24.0 mg, 0.10

mmol, 3 equiv) and toluene (4 mL). The reaction mixture was stirred at 150 °C for 6 h. The  
 crude material was purified using 35% acetone/hexanes. The desired product (20.0 mg, 0.02  
 mmol, 68% yield) was obtained as a dark blue solid. TLC (40% acetone/hexanes,  $R_f$  = 0.5);  
 mp 144-146 °C; IR (KBr, cm<sup>-1</sup>): 3351 (w), 2975 (w), 1739 (m), 1715 (m), 1694 (m), 1605  
 (m), 1577 (s), 1525 (w), 1510 (w), 1497 (w), 1468 (m), 1459 (m), 1416 (w), 1360 (s), 1293  
 (m), 1255 (m), 1159 (s), 1111 (s), 1001 (s), 860 (w), 814 (w), 801 (w), 754 (w), 721 (w), 699  
 (w), 558 (w), 528 (w); <sup>1</sup>H NMR (500 MHz, CDCl<sub>3</sub>): δ 7.59 (d,  $J$  = 8.7 Hz, 2H), 7.46 (d,  $J$  =  
 8.4 Hz, 2H), 7.37 (d,  $J$  = 1.6 Hz, 2H) 7.13 - 7.06 (m, 4H), 6.87 (s, 2H), 5.01 (d,  $J$  = 8.0 Hz,  
 2H), 4.60 (dd,  $J$  = 12.3, 5.6 Hz, 2H), 3.95 (s, 3H), 3.69 (s, 6H), 3.22 - 3.06 (m, 4H), 1.40 (s,  
 18H). <sup>13</sup>C {<sup>1</sup>H} (126 MHz, CDCl<sub>3</sub>): δ 172.4, 167.4, 161.8, 160.1, 155.2, 145.8, 134.5, 132.8,  
 132.5, 127.6, 125.7, 122.2, 121.9, 118.7, 117.9, 114.2, 113.0, 80.2, 55.7, 54.8, 52.5, 38.6,  
 28.4. HRMS (ESI+)  $m/z$  calcd for  $C_{46}H_{48}BF_2N_4O_{11}$  [M+H]<sup>+</sup> 881.3383. Found 881.3378.



**Synthesis of 42.** According to  
 GP3. **40** (32.0 mg, 0.03 mmol),

1  
2  
3 Pd(OAc)<sub>2</sub> (0.4 mg, 1.61 x 10<sup>-3</sup> mmol, 0.05 equiv), PPh<sub>3</sub> (0.8 mg, 3.2 x 10<sup>-3</sup> mmol, 0.1 equiv),  
4  
5 K<sub>2</sub>CO<sub>3</sub> (13.4 mg, 0.10 mmol, 3 equiv) and toluene (4 mL). The reaction mixture was stirred  
6  
7 at 150 °C for 6 h. The crude material was purified using 60% CHCl<sub>3</sub>/hexanes. The desired  
8  
9 product (9.1 mg, 0.01 mmol, 34% yield) was obtained as a blue solid. TLC (50%  
10  
11 acetone/hexanes, R<sub>f</sub> = 0.6); mp >300 °C decompose; IR (KBr, cm<sup>-1</sup>): 2930 (w), 2864 (w),  
12  
13 1738 (m), 1606 (w), 1574 (m), 1454 (m), 1417 (w), 1362 (s), 1338 (s), 1289 (m), 1254 (w),  
14  
15 1183 (m), 1114 (s), 996 (m), 983 (s), 974 (s), 906 (w), 892 (w), 877 (w), 758 (w), 737 (w),  
16  
17 702 (w), 666 (w), 583 (w); <sup>1</sup>H NMR (500 MHz, CD<sub>2</sub>Cl<sub>2</sub>-CDCl<sub>3</sub>): δ 7.61 (d, *J* = 8.4 Hz, 2H),  
18  
19 7.56 (s, 2H), 7.27 (s, 2H), 7.11 (d, *J* = 8.4 Hz, 2H), 6.85 (s, 2H), 3.94 (s, 3H), 3.07 - 3.01 (m,  
20  
21 4H), 2.52 - 2.32 (m, 6H), 2.18 - 2.02 (m, 7H), 2.02 - 1.88 (m, 3H), 1.69 - 1.57 (m, 6H), 1.56  
22  
23 - 1.39 (m, 6H), 0.91 (s, 6H). <sup>13</sup>C {<sup>1</sup>H} (126 MHz, CD<sub>2</sub>Cl<sub>2</sub>-CDCl<sub>3</sub>): δ 221.0, 167.9, 162.2,  
24  
25 160.0, 145.4, 137.4, 136.9, 134.8, 133.0, 126.3, 119.8, 118.9, 118.7, 118.3, 114.6, 113.1,  
26  
27 56.2, 51.2, 48.5, 45.0, 38.7, 36.5, 32.3, 30.9, 27.0, 26.8, 22.2, 14.4. HRMS (ESI+) *m/z* calcd  
28  
29 for C<sub>52</sub>H<sub>50</sub>BF<sub>2</sub>N<sub>2</sub>O<sub>5</sub> [M+H]<sup>+</sup> 831.3784. Found 831.3773.  
30  
31  
32  
33  
34  
35  
36  
37  
38  
39  
40

### 41 Supporting information:

42  
43 <sup>1</sup>H and <sup>13</sup>C NMR spectra of the compounds prepared. . Absorption and fluorescence spectra.  
44  
45 Cyclic voltammograms. Correlation of the fluorescence efficiency with solvent scales.  
46  
47 Photophysical and laser data. Crystallographic data by X-ray diffraction. XYZ coordinates  
48  
49 and energies of the simulated geometries.  
50  
51

52 The Supporting Information is available free of charge on the ACS Publications website at  
53  
54 DOI: xxxxx  
55  
56  
57  
58  
59  
60

**Author information:****Corresponding Author:**

\*Email: jorge.banuelos@ehu.eus, eduardop@ugto.mx

**ORCID**

Eduardo Peña-Cabrera: 0000-0002-2069-6178

José L. Belmonte-Vázquez: 0000-0002-1052-5260

Edurne Avellanal-Zaballa: 0000-0002-5218-3764

Ernesto Enríquez-Palacios 0000-0001-7270-2544

Luis Cerdán: 0000-0002-7174-2453

Ixone Esnal: 0000-0001-9625-6876

Jorge Bañuelos: 0000-0002-8444-4383

Clarisa Villegas-Gómez: 0000-0003-3221-1809

Iñigo López Arbeloa: 0000-0002-8440-6600

**Notes**

The authors declare no competing financial interest.

**Acknowledgements**

We gratefully acknowledge the Spanish Ministerio de Economía y Competitividad (MAT2017-83856-C3-3-P) and Gobierno Vasco (project IT912-16) for financial support. E. A.-Z. thanks also Gobierno Vasco for a predoctoral fellowship. The authors thank SGIker of UPV/EHU for technical and human support with the X-ray diffraction measurements and computational calculations, which were carried out in the “arina” informatic cluster. J.L.B.-V. and E.E.-P. thank CONACyT for scholarships. CONACyT (grants 253623, 123732) is acknowledged. Donation of 8-methylthioBODIPY by Cuantico de Mexico ([www.cuantico.mx](http://www.cuantico.mx)) is appreciated.

## References

- (1) (a) Molecular Probes Inc., Eugene, Oregon, USA. (b) R. P. Haugland, *The Handbook. A Guide to Fluorescent Probes and Labeling Technologies*, 10th edn. Molecular Probes Inc., Eugene, Oregon, USA.
- (2) Bañuelos, J. BODIPY Dye, the Most Versatile Fluorophore Ever? *Chem. Rec.* **2016**, *16*, 335-348.
- (3) (a) Loudet, A.; Burgess, K. BODIPY Dyes and Their Derivatives: Syntheses and Spectroscopic Properties. *Chem. Rev.* **2007**, *107*, 4891-4932. (b) Wood, T. E.; Thompson, A. Advances in the Chemistry of Dipyrins and Their Complexes. *Chem. Rev.* **2007**, *107*, 1831-1861.
- (4) (a) Ulrich, G.; Ziessel, R.; Harriman, A. The Chemistry of Fluorescent Bodipy Dyes: Versatility Unsurpassed. *Angew. Chem. Int. Ed.* **2008**, *47*, 1184-1201. (b) Boens, N.; Verbelen, B.; Dehaen, W. Postfunctionalization of the BODIPY Core: Synthesis and Spectroscopy. *Eur. J. Org. Chem.* **2015**, 6577-6595. (c) Lakshmi, V.; Sharma, R.; Ravikanth, M. Functionalized Boron-Dipyrromethenes and Their Applications. *Rep. Org. Chem.* **2016**, *6*, 1-24.
- (5) (a) Li, L.; Han, J.; Nguyen, B.; Burgess, K. Syntheses and Spectral Properties of Functionalized, Water-Soluble BODIPY Derivatives. *J. Org. Chem.* **2008**, *73*, 1963-1970. (b) Poirel, A.; Retailleau, P.; De Nicola, A.; Ziessel, R. Synthesis of Water-Soluble Red-Emitting Thienyl-BODIPYs and Bovine Serum Albumin Labeling. *Chem. Eur. J.* **2014**, *20*, 1252-1257. (c) Brellier, M.; Duportail, G.; Baati, R. Convenient Synthesis of Water-Soluble Nitrilotriacetic Acid (NTA) BODIPY Dyes. *Tetrahedron Lett.* **2010**, *51*, 1269-1272.

- 1  
2  
3 (6) Lakshmi, V.; Rao, M. R.; Ravikanth, M. Halogenated Boron-Dipyrromethenes:  
4 Synthesis, Properties and Applications. *Org. Biomol. Chem.* **2015**, *13*, 2501–2517.  
5  
6  
7 (7) Bessette, A.; Hanan, G. S. Design, Synthesis and Photophysical Studies of  
8 Dipyrromethene-Based Materials: Insights into Their Applications in Organic Photovoltaic  
9 Devices. *Chem. Soc. Rev.* **2014**, *43*, 3342-3405.  
10  
11  
12 (8) Benstead, M.; Mehl, G. H.; Boyle, R. W. 4,4'-Difluoro-4-Bora-3a,4a-Diaza-S-Indacenes  
13 (BODIPYs) as Components of Novel Light Active Materials. *Tetrahedron* **2011**, *67*, 3573-  
14 3601.  
15  
16  
17 (9) Ziessel, R.; Ulrich, G.; Harriman, A. The Chemistry of Bodipy: A New El Dorado for  
18 Fluorescence Tools. *New J. Chem.* **2007**, *31*, 496–501.  
19  
20  
21 (10) Singh, S. P.; Gayathri, T. Evolution of BODIPY Dyes as Potential Sensitizers for  
22 Dye-Sensitized Solar Cells. *Eur. J. Org. Chem.* **2014**, 4689-4707.  
23  
24  
25 (11) Benniston, A. C.; Copley, G. Lighting the Way Ahead with Boron Dipyrromethene  
26 (Bodipy) Dyes. *Phys. Chem. Chem. Phys.* **2009**, *11*, 4124-4131.  
27  
28  
29 (12) (a) Kamkaew, A.; Lim, S. H.; Lee, H. B.; Kiew, L. V.; Chung, L. Y.; Burgess, K.  
30 BODIPY Dyes in Photodynamic Therapy. *Chem. Soc. Rev.* **2013**, *42*, 77-88. (b) Awuahab,  
31 S. G.; You, Y. Boron Dipyrromethene (BODIPY)-Based Photosensitizers for Photodynamic  
32 Therapy. *RSC Adv.* **2012**, *2*, 11169–11183.  
33  
34  
35 (13) Lavis, L. D.; Raines, R. T. Bright Ideas for Chemical Biology. *ACS Chem. Biol.* **2008**,  
36 *3*, 142-155.  
37  
38  
39 (14) Husen Alamudi, S.; Satapathy, R.; Kim, J.; Su, D.; Ren, H.; Das, R.; Hu, L.; Alvarado-  
40 Martínez, E.; Lee, J. Y.; Hoppmann, C.; Peña-Cabrera, E.; Ha, H.-H.; Park, H.-S.; Wang, L.;  
41 Chang, Y.-T. Development of background-free “Tame” fluorescent probes for intracellular  
42 live cell imaging *Nat. Commun.* **2017**, *7*, 1-9.  
43  
44  
45  
46  
47  
48  
49  
50  
51  
52  
53  
54  
55  
56  
57  
58  
59  
60

- 1  
2  
3 (15) Lu, H.; Mack, J.; Yang, Y.; Shen, Z. Structural Modification Strategies for the Rational  
4 Design of Red/NIR Region BODIPYs. *Chem. Soc. Rev.* **2014**, *43*, 4778-4823.  
5  
6  
7 (16) Fayed, T. A. Extension of Fluorescence Response to the Near-IR Region, in *Reviews in*  
8 *Fluorescence*, 75-111, Ed. Geddes, C. D., Springer, **2009**.  
9  
10  
11 (17) Shindy, H. A. Fundamentals in the Chemistry of Cyanine Dyes: A Review. *Dyes and*  
12 *Pigments* **2017**, *145*, 505-513.  
13  
14  
15 (18) Sauer, M.; Hofkens, J.; Enderlein, J. *Handbook of Fluorescence Spectroscopy and*  
16 *Imaging*. 2010, Wiley-VCH, Weinheim, Germany.  
17  
18  
19 (19) Dou, L.; Liu, Y.; Hong, Z.; Li, G.; Yang, Y. Low-Bandgap Near-IR Conjugated  
20 Polymers/Molecules for Organic Electronics *Chem. Rev.* **2015**, *115*, 12633-12665.  
21  
22  
23 (20) Nia, Y.; Wu, J. Far-Red and Near Infrared BODIPY Dyes: Synthesis and Applications  
24 for Fluorescent pH Probes and Bio-Imaging *Org. Biomol. Chem* **2014**, *12*, 3774-3791.  
25  
26  
27 (21) Awuahab, S. G.; You, Y. Boron Dipyrromethene (BODIPY)-Based Photosensitizers for  
28 Photodynamic Therapy *RSC Adv.* **2012**, *2*, 11169–11183.  
29  
30  
31 (22) You, Y.; Nam, W. Designing Photoluminescent Molecular Probes for Singlet Oxygen,  
32 Hydroxyl Radical, and Iron–oxygen Species. *Chem. Sci.* **2014**, *5*, 4123-4135.  
33  
34  
35 (23) (a) Zeng, L.; Jiao, C.; Huang, X.; Huang, K.-W.; Chin, W.-S.; Wu, J. Anthracene-Fused  
36 BODIPYs as Near-Infrared Dyes with High Photostability. *Org. Lett.* **2011**, *13*, 6026-6029.  
37  
38 (b) Jiao, C.; Huang, K.-W.; Wu, J. Perylene-Fused BODIPY Dye with Near-IR  
39 Absorption/Emission and High Photostability. *Org. Lett.* **2011**, *13*, 632-635.  
40  
41  
42 (24) Shen, Z.; Röhr, H.; Rurack, K.; Uno, H.; Spieles, M.; Schulz, B.; Reck, G.; Ono, N.  
43 Boron–Diindomethene (BDI) Dyes and Their Tetrahydrobicyclo Precursors-en Route to a  
44 New Class of Highly Emissive Fluorophores for the Red Spectral Range. *Chem. Eur. J.* **2004**,  
45 *10*, 4853-4871.  
46  
47  
48  
49  
50  
51  
52  
53  
54  
55  
56  
57  
58  
59  
60

1  
2  
3 (25) Jiao, L.; Yu, C.; Liu, M.; Wu, Y.; Cong, K.; Meng, T.; Wang, Y.; Hao, E. Synthesis and  
4 Functionalization of Asymmetrical Benzo-Fused BODIPY Dyes. *J. Org. Chem.* **2010**, *75*,  
5 6035–6038.  
6  
7

8  
9  
10 (26) Okujima, T.; Tomimori, Y.; Nakamura, J.; Yamada, H.; Uno, H.; Ono, N. Synthesis of  
11  $\pi$ -Expanded BODIPYs and Their Fluorescent Properties in the Visible-near-infrared Region.  
12  
13 *Tetrahedron* **2010**, *66*, 6895-6900.  
14  
15

16  
17 (27) Heyer, E.; Retailleau, P.; Ziessel, R.  $\alpha$ -Fused Dithienyl BODIPYs Synthesized by  
18 Oxidative Ring Closure. *Org. Lett.* **2014**, *16*, 2330-2333.  
19  
20

21 (28) Hayashi, Y.; Obata, N.; Tamaru, M.; Yamaguchi, S.; Matsuo, Y.; Saeki, A.; Seki, S.;  
22 Kureishi, Y.; Saito, S.; Yamaguchi, S.; Shinokubo, H. Facile Synthesis of Biphenyl-Fused  
23 BODIPY and Its Property. *Org. Lett.* **2012**, *14*, 866-869.  
24  
25  
26

27 (29) Kubo, Y.; Minowa, Y.; Shoda, T.; Takeshita, K. Synthesis of a New Type of  
28 Dibenzopyrromethene-boron Complex with Near-Infrared Absorption Property.  
29  
30  
31  
32  
33 *Tetrahedron Lett.* **2010**, *51*, 1600–1602.  
34

35 (30) Ni, Y.; Wu, J. Far-Red and near Infrared BODIPY Dyes: Synthesis and Applications for  
36 Fluorescent pH Probes and Bio-Imaging *Org. Biomol. Chem.* **2014**, *12*, 3774-3791.  
37  
38

39 (31) (a) Umezawa, K.; Nakamura, Y.; Makino, H.; Citterio, D.; Suzuki, K. Bright, Color-  
40 Tunable Fluorescent Dyes in the Visible-Near-Infrared Region. *J. Am. Chem. Soc.* **2008**, *130*,  
41 1550-1551. (b) Umezawa, K.; Matsui, A.; Nakamura, Y.; Citterio, D.; Suzuki, K. Bright,  
42 Color-Tunable Fluorescent Dyes in the Vis/NIR Region: Establishment of New “Tailor-  
43 Made” Multicolor Fluorophores Based on Borondipyrromethene. *Chem. Eur. J.* **2009**, *15*,  
44 1096-1106.  
45  
46  
47  
48  
49  
50  
51  
52  
53  
54  
55  
56  
57  
58  
59  
60

1  
2  
3 (32) Leen, V.; Qin, W.; Yang, W.; Cui, J.; Xu, C.; Tang, X.; Liu, W.; Robeyns, K.; Van  
4 Meervelt, L.; Beljonne, D.; Lazzaroni, R.; Tonnel, C.; Boens, N.; Dehaen, W. Synthesis,  
5 Spectroscopy, Crystal Structure Determination, and Quantum Chemical Calculations of  
6 BODIPY Dyes with Increasing Conformational Restriction and Concomitant Red-Shifted  
7 Visible Absorption and Fluorescence Spectra. *Chem. Asian J.* **2010**, *5*, 2016-2026.

8  
9  
10  
11  
12  
13  
14 (33) Gómez-Durán, C. F. A.; Esnal, I.; Valois-Escamilla, I.; Urías-Benavides, A.; Bañuelos,  
15 J.; López Arbeloa, I.; García-Moreno, I.; Peña-Cabrera, E. Near-IR BODIPY Dyes á la Carte-  
16 Programmed Orthogonal Functionalization of Rationally Designed Building Blocks. *Chem.*  
17 *Eur. J.* **2016**, *22*, 1048-1061.

18  
19  
20  
21  
22  
23 (34) (a) Prokopcová, H.; Kappe, C. O. The Liebeskind–Srogl C-C Cross-Coupling Reaction.  
24 *Angew. Chem. Int. Ed.* **2009**, *48*, 2276-2286. (b) Cheng, H.-G.; Chen, H.; Liu, Y.; Zhou, Q.  
25 The Liebeskind–Srogl Cross-Coupling Reaction and its Synthetic Applications. *Asian J. Org.*  
26 *Chem.* **2018**, *7*, 490-508.

27  
28  
29  
30  
31  
32 (35) (a) Jones II, G.; Huang, Z.; Kumar, S.; Pacheco, D. Fluorescence and Lasing Properties  
33 of Benzo-Fused Pyrromethene Dyes in Poly(methyl methacrylate) Solid Host Media. *SPIE -*  
34 *Int. Soc. Opt. Eng.* **2002**, *4630*, 72-81. (b) Jones II, G.; Huang, Z.; Pacheco, D. Fluorescence  
35 and Lasing Properties of Meso-Substituted Benzo-Fused Pyrromethene Dyes in Solid Media.  
36 *SPIE - Int. Soc. Opt. Eng.* **2003**, *4968*, 24-34.

37  
38  
39  
40  
41  
42 (36) Zeni, G.; Larock, R. C. Synthesis of Heterocycles via Palladium-Catalyzed Oxidative-  
43 Addition. *Chem Rev.* **2006**, *106*, 4644-4680.

44  
45  
46  
47  
48  
49 (37) Jiang, T.; Zhang, P.; Yu, C.; Yin, J.; Jiao, L.; Dai, E.; Wang, J.; Wei, Y.; Mu, X.; Hao,  
50 E. Straightforward Synthesis of Oligopyrroles through a Regioselective S<sub>N</sub>Ar Reaction of  
51 Pyrroles and Halogenated Boron Dipyrins. *Org. Lett.* **2014**, *16*, 1952–1955.  
52  
53  
54  
55  
56  
57  
58  
59  
60

1  
2  
3 (38) Isomer **3** was prepared in two steps; the first arylation reaction took place in refluxing  
4 dioxane for 96 h, while the second arylation took place in refluxing toluene for 48 h (see ref.  
5  
6  
7  
8 32).

9  
10 (39) Chen, J.; Burghart, A.; Derecskei-Kovacs, A.; Burgess, K. 4,4-Difluoro-4-bora-3a,4a-  
11 diaza-*s*-indacene (BODIPY) Dyes Modified for Extended Conjugation and Restricted Bond  
12 Rotations. *J. Org. Chem.* **2000**, *65*, 2900–2906.  
13  
14

15  
16 (40) Kee, H. L.; Kirmaier, C.; Yu, L.; Thamyongkit, P.; Youngblood, W. J.; Calder, M. E.;  
17 Ramos, L.; Noll, B. C.; Bocian, D. F.; Scheidt, W. R.; Birge, R. R.; Lindsey, J. S.; Holten,  
18 D. Structural Control of the Photodynamics of Boron-Dipyrroin Complexes. *J. Phys. Chem.*  
19 *B* **2005**, *109*, 20433-20443.  
20  
21

22 (41) Luo, L.; Wu, D.; Li, W.; Zhang, S.; Ma, Y.; Yan, S.; You, J. Regioselective  
23 Decarboxylative Direct C–H Arylation of Boron Dipyrromethenes (BODIPYs) at 2,6-  
24 Positions: A Facile Access to a Diversity-Oriented BODIPY Library. *Org. Lett.* 2014, *16*,  
25 6080-6083.  
26  
27

28 (42) Reichardt, C. Solvatochromic Dyes as Solvent Polarity Indicators. *Chem. Rev.* **1994**, *94*,  
29 2319-2358.  
30  
31

32 (43) García-Moreno, I., Costela, A., Martín, V. Pintado-Sierra, M., Sastre, R. Materials for a  
33 Reliable Solid-state Dye Laser at the Red Spectral Edge. *Adv. Funct. Mater.* **2009**, *19*, 2547-  
34 2552.  
35  
36

37 (44) Durán-Sampedro, G.; Agarrabeitia, A. R.; Cerdán, L.; Pérez-Ojeda, M. E.; Costela, A.;  
38 García-Moreno, I.; Esnal, I., Bañuelos, J.; López-Arbeloa, I.; Ortiz, M. J. Carboxylates vs  
39 Fluorines: Boosting the Emission Properties of Commercial BODIPYs in Liquid and Solid  
40 Media. *Adv. Funct. Mater.* **2013**, *23*, 4195-4205.  
41  
42  
43  
44  
45  
46  
47  
48  
49  
50  
51  
52  
53  
54  
55  
56  
57  
58  
59  
60

1  
2  
3 (45) (a) Masilamani, V.; Aldwayyan, A. S. Structural and Solvent Dependence of  
4 Superexciplex. *Spectrochim. Acta Part A* **2004**, *60*, 2099-2106. (b) Cerdán, L, Martínez-  
5 Martínez, V.; García-Moreno, I.; Costela, A.; Pérez-Ojeda, M. E.; López-Arbeloa, I.; Wu,  
6 L.; Burgess, K. Naturally Assembled Excimers in Xanthenes as Singular and Highly Efficient  
7 Laser Dyes in Liquid and Solid Media. *Adv. Opt. Mater.* **2013**, *1*, 984-990.

8  
9  
10  
11  
12 (46) Cerdán, L.; Costela, A.; García-Moreno, I.; Bañuelos, J.; López-Arbeloa, I. Singular  
13 Laser Behaviour of Hemycyanine Dyes: Unsurpassed Efficiency and Finely Structured  
14 Spectrum in the Near-IR Region. *Laser Phys. Lett.* **2012**, *9*, 426-433.

15  
16  
17 (47) Durán-Sampedro, G.; Agarrabeitia, A. R.; Arbeloa, T.; Bañuelos, J.; López-Arbeloa, I.;  
18 Chiara, J. L.; Garcia-Moreno, I.; Ortiz, M. J. Increased Laser Action in Commercial Dyes  
19 from Fluorination Regardless of their Skeleton. *Laser Phys. Lett.* **2014**, *11*, 115818.

20  
21  
22 (48) Jones II, G.; Kumar, S.; Klueva, O.; Pacheco, D. Photoinduced Electron Transfer for  
23 Pyrromethene Dyes. *J. Phys. Chem. A* **2003**, *107*, 8429-8434.

24  
25  
26 (49) Lakshmi, V.; Ravikanth, M. Synthesis of Hexasubstituted Boron-Dipyrromethenes  
27 Having a Different Combination of Substituents. *Eur. J. Org. Chem.* **2014**, 5757-5766.

28  
29  
30 (50) Jiao, L.; Pang, W.; Zhou, J.; Wei, Y.; Mu, X.; Bai, G.; Hao, E. Regioselective Stepwise  
31 Bromination of Boron Dipyrromethene (BODIPY) Dyes *J. Org. Chem.* **2011**, *76*, 9988-9996.

32  
33  
34  
35  
36  
37  
38  
39  
40  
41  
42  
43  
44  
45  
46  
47  
48  
49  
50  
51  
52  
53  
54 TOC

